Thermal and Hydraulic Modeling and Control of a District Heating System

Kang Xu

A Thesis in

The Department of Building, Civil and Environmental Engineering

Presented in Partial Fulfillment of the Requirements

For the Degree of Master of Applied Science at

Concordia University

Montreal, Quebec, Canada

October 2012

CONCORDIA UNIVERSITY

School of Graduate Studies

This is to certify that the thesis prepared

By: Kang Xu

Entitled: Thermal and Hydraulic Modeling and Control of a District Heating System

and submitted in partial fulfillment of the requirements for the degree of

Master of Applied Science

complies with the regulations of the University and meets the accepted standards with respect to originality and quality.

Signed by the final examining committee:

Dr. L. Wang	Chair
Dr. L. Lopes	External Examiner
Dr. Z. Chen	Examiner
Dr. L. Wang	Examiner
Dr. M. Zaheer-uddin	Thesis Supervisor

Approved by: _____

Chair of Department or Graduate Program Director

December 10 2012 _____

Dean of Faculty

ABSTRACT

Thermal and Hydraulic Modeling and Control of a District Heating System

Kang Xu

A district heating system is a centralized heating system widely used for space heating. They offer economic benefits and are acknowledged to be more energy efficient. Their energy efficiency can be further improved by optimally controlling and operating the overall system. With this as the motivation a thermal and hydraulic model of a district heating is developed in this thesis.

The developed model consists of a boiler, six buildings, hot water distribution network, circulating pump, balancing and control valves and terminal heaters. Both dynamic and steady state hydraulic simulations were made to study supply, return water and zone temperature response; Pressure distribution in the piping network under different load conditions. A relationship between balance valve settings and outdoor temperature (heating load) was determined. It was shown that proper setting of balance valves as a function of heating load improves energy efficiency.

Proportional-Integral (PI) controllers were designed for the boiler and zone temperature control. Closed loop simulations are presented to show the control performance. By using steady state optimization technique optimal set points for the boiler temperature and near-optimal balance valve positions as a function of outdoor temperature were determined.

Simulation results show that the use of optimal set points and balance valve settings up to 20% energy can be saved compared to the conventional outdoor air reset control strategy. Simulation results under different operating conditions are presented.

ACKNOWLEDGEMENTS

I would like to express my sincere gratitude to my supervisor Dr. Mohammed Zaheer-uddin for his sustained guidance and assistance during the whole span of this research work.

My thanks are also to the members of staff in Concordia University for their kind help whenever I need. Especially thanks go to Dr. Lianzhong Li and Mr. Songchun Li for their helpful work.

I would like to dedicate this thesis to my wife, Ying Lu and my lovely daughter, Yawan Xu, for their patience, understanding and support during my whole studies.

TABLE OF CONTENTS

LIST OF FIGURES

LIST OF TABLES

LIST OF SYMBOLS

Capital letters

A_{di} Heated Floor Area (m^2)

C_b Thermal capacity of boiler (J/℃)

$C_{htr1\sim6}$ Thermal capacity of heaters (J/℃)

$C_{iwl(s,e,w,n)(1,2,3,4)}$ Thermal capacity of 1,2,3,4 layers on the south, east, west or north wall of building *i* (J/℃)

D_h Hydraulic diameter of pipe segment (m)

D_o Outside diameter of pipe with insulation (m)

D_{ii} Outside diameter of pipe without insulation (m)

G_{cp} Water mass flow rate of each pipe (kg/s)

G_{mk} The mass flow rate of makeup water (kg/s)

G_p Water mass flow rate of pump (kg/s)

HV Heat value of the fuel (MJ/kg)

H_{emb} Average height of embedded pipe (m)

H_{req} The required water pressure head of circulating pump (Pa)

K The absolute roughness of inside pipe wall (m)

L_{dp} The equivalent length of pipe (m)

L_p Average pitch between supply and return pipe (m)

PD_{bvi} The pressure drop on balance valve *i* (Pa)

PD_{bvirat} Normally ratio of pressure drop on the balance valve *i* to branch loop (dimensionless)

PD_{bvisp} The pressure drop set point of balance valve *i* (Pa)

P_{Hpump} The pressure head of circulating pump (Pa)

P_v Vapor pressure of water saturation at current temperature (Pa)

Q_{di} Heating load for building *i* (W)

Q_{gain} Zone heat gain from solar radiation and internal heat resources (W)

Q_{lsi} The heat lost from pipe segment i (W)

$Q_{solwl(s,e,w,)i}$ Heat gain from solar of south, east or west wall of building *i* (W)

R_{cp} The friction rate of pipe (Pa/m)

R_e Reynolds Number (dimensionless)

R_{insi} The thermal resistance of insulation of pipe segment i (m℃/W)

R_{int} Additional thermal resistance between supply and return pipe segment (m℃/W)

R_{pi} The ratio of water resistance of the pipe segment i (Pa/m)

R_{soili} The thermal resistance of soil to pipe segment i (m℃/W)

T_b The output water temperature from boiler (℃)

T_{bsp} Water temperature set point of boiler (℃)

T_{mk} Makeup water temperature (℃)

T_o Outdoor air temperature (℃)

T_{od} Design outdoor air temperature (℃)

T_r The return water temperature (℃)

T_{rd} Design return water temperature (℃)

T_s Supply water temperature (℃)

T_{sd} Design supply water temperature (℃)

T_{soil} Average surface temperature of ground (℃)

T_z Indoor air temperature (℃)

T_{zd} Design indoor air temperature (℃)

U_{eni} Overall heat transfer coefficient for each building enclosure (W/℃)

$U_{htr1\sim6}$ Actual heat transfer coefficient of heaters 1~6 (W/m^2)

U_{iwlo1} Overall heat-transfer coefficients of exterior wall nodes from the outside to layer 1of the building i (W/m^2℃)

U_{iwl12} Overall heat-transfer coefficients of exterior wall nodes from layer 1 to layer 2 of the building i (W/m^2℃)

U_{iwl23} Overall heat-transfer coefficients of exterior wall nodes from layer 2 to layer 3 of the building i (W/m^2℃)

U_{iwl34} Overall heat-transfer coefficients of exterior wall nodes from layer 3 to layer 4 of the building i (W/m^2℃)

U_{iwl4i} Overall heat-transfer coefficients of exterior wall nodes from layer 4 to inside of the building i (W/m^2℃)

V Water flow velocity (m/s)

WR_i Water resistance of pipe segment i (Pa)

WR_{ui} The water resistance of terminal heater i (Pa)

WR_{cvi} The water resistance of control valve i (Pa)

WR_b The water resistance of boiler (Pa)

X_F Operating pressure ratio (dimensionless)

ΔP_b The friction resistance of boiler (Pa)

ΔP_{bd} Water resistance of boiler (Pa)

ΔP_{ip} The friction resistance of pipe segment (Pa)

ΔP_u The friction resistance of building (Pa)

ΔP_{ui} Water resistance of user *i* (Pa)

ΔP_v The friction resistance of control valve (Pa)

Small letters

c_i The modified index for heat transfer coefficient of heater (dimensionless)

c_w Specific heat of water (J/Kg℃)

c_z Specific heat of air (J/Kg℃)

$c_{1\sim6}$ The modified index for heat transfer coefficient (dimensionless)

d_p Diameter of pipe (m)

e_b The efficiency of boiler (dimensionless)

e_{motor} The efficiency of electric motor (dimensionless)

e_{pump} The efficiency of circulating pump (dimensionless)

$f_{1\sim6}$ The safety factor for heat transfer area of heater (dimensionless)

f_g The safety factor for circulating water flow rate (dimensionless)

f_f The safety factor of circulating pump in flow rate (dimensionless)

f_m The safety factor of makeup water pump in flow rate (dimensionless)

f_{mp} The safety factor of makeup water pump in pressure head (dimensionless)

f_r The safety factor of circulating pump in pressure head (dimensionless)

h_{soil} Heat transfer coefficient of air on the surface of the ground (W/ m^2℃)

k_i The integral gain (dimensionless)

k_{insp} Thermal conductivity of pipe insulation (W/ m℃)

k_p The proportional gain (dimensionless)

k_{soil} Conductivity of soil (W/ m℃)

m_{bd} Hot water capacity of boiler (t/h)

$m_{f\max}$	The maximum mass flow rate of fuel (kg/s)
m_i	The water mass flow rate in pipe segment *i* (Kg/s)
q_d	Heating load Index (W/m^2)
u_f	Fuel flow rate control variable of boiler (dimensionless)
u_{bvi}	Normalized flow rate in balance valve *i* (dimensionless)
u_{bvri}	The ratio of balance valve *i* opening (dimensionless)
u_{cvi}	Normalized flow rate in control valve *i* (dimensionless)
u_w	Control variable of valve normalized with respect to full open position (dimensionless)
u_{wi}	Normalized flow rate in the whole DH system (dimensionless)
ρ_w	Water density (Kg/m^3)
λ	Friction coefficient (dimensionless)
λ_{cp}	The friction factor of pipe (dimensionless)
μ	The dynamic viscosity at average temperature (Ns/m^2)
υ	The kinematic viscosity at average temperature (m^2/s)
α	The partial friction rate of pipe (dimensionless)
β	Heat loss factor by fittings (dimensionless)
$\eta_{b\max}$	The maximum efficiency of boiler (dimensionless)

Subscript

b	Referring to boiler
bv	Referring to balance valve
cv	Referring to control valve
d	Referring to design condition
e	Referring to east
f	Referring fuel
en	Referring to building enclosure
i	Referring to sequent number
in	Referring to insulation
ls	Referring to heat lost
m	Referring to makeup water
n	Referring to north
o	Referring to outdoor
r	Referring return water or rate
s	Referring to supply water or south
sol	Referring to solar
sp	Referring to set point

u	Referring to user
w	Referring to water or west
wl	Referring to building wall
z	Referring to zone

CHAPTER 1

Introduction

2.1 Introduction

A district heating system is a centralised heating system used for space heating to maintain acceptable temperature in a large network of buildings in a district area. The first district heating system was built at Lockport (New York, USA) in 1877. Since then its use has spread to many countries of Europe. [8] As central heating has (especially combined heat and power generation) obvious advantages such as saving energy, improving the environment and thermal comfort, the district heating system has been rapidly promoted and applied in latter half of last century.

There are several types of heating systems which are characterized by different heat sources, heating medium, terminal delivery and heat exchanger style. The most common district heating system is made up of one or more boilers, distribution pipeline network and terminal radiators. Besides, in order to effectively transfer and control the heating medium such as the hot water flowing in a closed loop, circulating pumps, balancing and control valves are necessary.

A district heating system is usually used in a large building or group of buildings and is widely used in residential, commercial and industry buildings. This thesis research is focused on the design and analysis of a district heating system which includes commercial and residential buildings.

A heating system is designed to satisfy heat transfer from boiler to user space. In this thermal energy transfer process, the dynamic variation of temperatures must be considered. The time response characteristics of building envelope from the enclosure elements will influence the thermal comfort level. In addition, the energy loss will also influence the performance of the system. A dynamic simulation model is required to study these effects.

Flow balancing is indispensable in a DH system. A correct set of balance valves can ensure the correct distribution in whole system that corresponds to the design flow rates. A standard practice nowadays in district heating system design is the constant flow system design. These systems are balanced by using a proportional method with manual reset. Also, fixed-orifice, double-regulating balance valves are installed to account for and reduce the impact of pressure changes in the system. Since these systems rarely operate at full load, the normal practice of leaving the balance valve settings at their design settings results in higher pump energy consumption. In this sense it is important to study the use of innovative approaches to control the balance valves as proposed in this thesis.

In this thesis, a dynamic model of the district heating system, including sub-system models of boiler, distribution system, piping network, environmental zones and terminal heaters will be developed.

Both open loop and closed loop operation of the DH system will be studied by carrying out simulation runs. An energy optimal control strategy which will minimize boiler

energy consumption and pumping energy costs will be developed and tested through simulation runs conducted over a wide range of weather and operating conditions.

CHAPTER 2

Literature Review

A literature survey related to system design, operation, dynamic model, hydraulic balance, control strategies and optimal operation of district heating (DH) system is presented below. The literature review findings are described in the following sub-sections.

2.1 A review of DH system dynamic models

A dynamic model is essential for simulation and control to study energy efficiency of district heating systems. It is usually consisted of several component models such as boiler, distribution network, single or multi-zone, building enclosure, and terminal heaters.

Zaheer-uddin and Monastiriakos (1998) [19] developed two dynamic models of general domestic hydraulic heating system both space heating and domestic hot water respectively. Energy balance approach was used to develop sub-system models such as boiler, baseboard heater and environmental zone. The model of terminal baseboard unit was based on the energy balance equations between hot water in the tubes and the fin-tube metal surface. The temperature responses show the model equations and parameters used are suitable for simulation studies and those models were validated by using field measurement data.

Li (2003) [10] developed a typical dynamic model of a district heating system which supplied heating for 30 buildings. It included aggregated building, boiler, zone, terminal

heater, supply and return water temperature sub-system models. Solar radiation and internal heat load were utilized as disturbance to simulate real operating conditions. The method of multi-variable optimization was used to optimize operating parameters of DH system in order to minimize system operating cost. A reduced-order model was described and used for the design of a Smith Predictor in order to improve the system performance, especially disturbance rejection. The result showed that energy consumption could be reduced up to 25% by using optimal set points to operate the boiler compared with conventional approach of using arbitrary set points. Furthermore, it was shown that optimal control strategy combined with a Smith Predictor controller could give superior performance in terms of temperature regulation and disturbance rejection.

From what is stated above, it may be concluded that supply water temperature control has a significant importance on control performance and energy saving of DH system. However, the water mass flow rate is also an important factor that may influence the control performance and energy saving of the whole system.

Z. Liao and A.L. Dexter (2003) [29] used a simulation to study the impacts of boiler control on the overall performance of multi-zone heating system. An inferential control scheme method was used to optimize the operation of boilers in multi-zone heating system where there was no measurement of internal air temperature. By using the output of estimator which estimated experimental data obtained from different available information to feedback PI controller of boiler, the hot water supply temperature set point was determined. The simulation results showed that the inferential control scheme could reduce the energy consumption and improve the overall control performance in the thermal comfort of buildings. After that, Z. Liao and A.L. Dexter (2004) [30] developed a

simplified physical model for estimating the average air temperature in multi-zone heating system in order to support the inferential boiler control scheme presented in [29].

Tianzhen Hong and Yi Jiang (1997) [22] presented a new multi-zone model with an improvement on the state space model, which had more efficiency in the simulation of large scale buildings than other methods. Based on a PC program known as BTP (Building Thermal Performance), this new multi-zone model was proposed to simulate energy performance of large scale building such as more than 200 zones to reduce computational time.

2.2 A review of DH system hydraulic network design and operation

In order to achieve as high as possible energy efficiency and low total cost of a DH system operation, it is necessary to optimize the various design and operating parameters, such as pipeline diameters, combinations of supply hot water temperatures and water mass flow rates, pump's operating characteristics and pressure head etc. Vladimir (2007) [24] presented an efficient method for numerical simulation and analyses of the steady state hydraulics of pipeline network. It is based on the loop model of the network and the method of square roots for solving the system of linear equations. The results show a potential for electricity savings in pump's operation.

Fu Lin and Jiang Yi (2001) [6] studied the influence of supply and return water temperature on the energy consumption of a district heating and cooling system. The paper analyzed the effect of the supply and return water temperature in the circulation network on the primary energy consumption of the system, which determined the

relationship between electricity consumption of circulating pump with the temperature difference of supply and return water in the network.

Baoping Xu, Lin Fu & Hongfa Di (2009) [2] explored the effects of consumer behavior on hydraulic performance and energy saving efficiency of a district heating system in China. A lot of field data was used to study the effects of consumer stochastic behavior such as regulation of TRVs (thermostatic radiator valves) and opening windows. The fluctuation of the whole DH system was less than 10% with a probability of 96.8%when the house-holders of the heating district reached 200. Usually, the effects would be decreased with increasing the number of terminal house-holders.

Kemal Comakli, Bedri Yuksel & Omer Comakli (2004) [8] studied the heat losses occurring in the district heating network system due to supply and return water temperatures. The analysis indicated that the heat losses in the network primarily dependent on the hot water temperature and thermal insulation thickness in pipes.

Nurdan Yildirim, Macit Toksoy, Gulden Gokcen (2010) [20] gave a design of piping network of a geothermal district heating system including design parameters of heat center location, target pressure loss, pipe materials and installation types and also evaluated the optimization of the network to minimize the total investment and operational cost.

M. Bojic, N. Trifunovic (2000) [17] presented improving thermal comfort of an unbalanced heat distribution in buildings in a district heating system by using bottom-up approach and sequential linear programming. Results showed that adjusting the valves of secondary pipe network and resizing substation heat exchanger might solve the problem.

Kyu Nam Rhee, Myoung Souk Yeo, Kwang Woo Kim (2011) [9] presented control performance evaluation of a hydraulic radiant heating system by using an emulation method. In the emulation, the equivalent hydraulic resistance was used to present the pressure loss and flow rate in hydraulic network instead of real pipe segment. The performance of several control strategies was evaluated based on this method by using real control system which connected hydraulic network and thermal model. The results showed that hydraulic balancing would improve the individual control performance and the hydraulic control device such as flow limit and pressure differential control valve could improve the accuracy of the temperature control. However, the system energy performance such as fuel and electrical power were not presented in this model.

Vladimir D. Stevanovic, Branislav Zivkovic, Sanja Prica, Blazenka Maslovaric,Vladan Karamarkovic, Vojin Trkulja (2009) [25] presented a dynamic model and numerical method to compute the thermal transient conditions in a district heating system. A steady-state hydraulic model was utilized to calculate network hydraulic parameters such as pressure and flow rate distribution in the pipe network within the periods of thermal transients. However, the optimal operation for improving energy efficiency of whole district heating system by combination of thermal transient conditions and hydraulic conditions were not examined in this paper.

Mauro Gamberi, Riccardo Manzini, Alberto Regattieri (2009) [16] presented an innovative technique for modeling a multi-zone hydraulic heating system. A Newton-Raphson Method was used to building the hydraulic heating system simulator in Matlab and Simulink environment to simulate both hydraulic and thermal behaviour of the heating system. Furthermore, a quasi-steady state approach named extended-period

simulation was used to simulate the system running sequence. With the hypothesis of mechanical and thermal exchanges occur independently, the model equations were solved, with hydraulic system as the input to the thermal system. The results showed that there was good agreement between measured and simulated data. However, the control strategy and optimization applied in this model for improving energy efficiency of the heating system was not discussed in the paper.

2.3 Effect of balancing valves on DH system

The balancing valves are necessary in order to balance the hydraulic water pressure distribution in the branch of pipe network to satisfy all heating needs of different branch users.

Takeyoshi Kimura, Takaharu Tanaka, K. F., K. O. (1995) [21] studied hydrodynamic characteristics of butterfly valves using theoretical prediction equations. The results agreed very well with the experimental data.

Shoukat Choudhury, Thornhillb, Shaha (2005) [12] developed a data-driven empirical friction model to present the control loop performance effected by control friction.

Claudio Garcia (2008) [4] studied the different friction models applied to control valves in order to analyze the effect due to the friction of the valves operating in control loops. These models were built on physical principles including the use of static and dynamic states and empirical data. By using different friction coefficients and signal inputs, the behavior of valves in different models was compared.

Kyu Nam Rhee, Myoung Souk Yeo, Kwang Woo Kim (2011) [9] developed an emulation method which by using real hardware to replace the hydraulic network to build a thermal-hydraulic integrated model. In this model, the balancing valve which had same hydraulic resistance as the real hydraulic circuit was used to replace the pipe section. The results showed that hydraulic balancing has to be combined with individual control in order to improve the control accuracy and control performance.

2.4 Control and operation strategies of DH system

Control and operation strategies are essential to improve thermal comfort and energy efficiency of DH systems.

Zaheer-uddin (1998) [19] developed a dynamic model of a hydraulic system to design feedback controllers and control strategies for the system. The performance of the feedback controller was compared with the two-position controller. A load-tracking set point control strategy was also presented by continuously matching the heating load with the burner capacity to achieve high overall boiler efficiency. Optimal boiler set point temperature was generated by using an outdoor air temperature reset strategy. The results showed that the designed controllers maintained the temperatures close to their set points in real operating conditions and the load matching control strategy gave good boiler temperature control performance.

Lianzhong and Zaheer-uddin (2008) [11] studied the dynamic responses of temperature and water mass flow rate in a hot water heating system for a high-rise building. Two

types of boiler temperature set-point strategies, one based on average outdoor air temperature method and the other using a fuzzy augmented system, were explored and their performance was compared. The simulation results show that the strategy based on the fuzzy augmented system could save boiler fuel consumption by 10%.

Liao, Swainson, Dexter (2005) [31] reviewed the current heating system control practice in the UK by surveys, computer simulations and experimental studies. Different boiler controllers and heat emitter controllers were studied to achieve energy saving with good zone temperature control. The results showed that using external temperature compensated controller was more efficient than a fixed temperature thermostat to maximize energy efficiency.

Baoping Xu, Lin Fu, Hongfa Di (2008) [3] developed a model to simulate the thermal and hydraulic behavior of space heating system with radiators controlled by thermostat valves for multi-zone building. This integrated model included two parts, one was the thermal system consisting of sub-models such as zone, radiators and TRVs, and other one was hydraulic network model for calculating water mass flow rate in each loop. Through a case study, the results showing the heat transport delay in the radiator, dynamic performance of zone, effect of TRV control and heat transfer between neighbors were presented. It also showed the influence of water flow rate on the control strategy of the heat supply station. However, though it presented the relationship between supply water temperature and water flow rate with the heat load changes, it didn't present how to optimize them and implement into control strategy.

Z. Liao, Dexter (2004) [28] presented investigation about boiler control types in current practice of district heating system. The data of survey demonstrated the problems associated with the boiler control strategies in district heating systems. The results showed that more than 20% energy savings and thermal comfort improvements would be achieved by using a better boiler control strategy.

Manohar R. Kulkarni, Feng Hong (2004) [14] compared the thermal comfort and energy efficiency between PI control and the traditional two-position control system for the residential building by setting up dynamic simulation. The comparative results showed that although there was not much difference in energy consumption, PI control scheme had much better performance than the two-position control system in thermal comfort. However, the relationship between boiler efficiency and the load should be considered when choosing a PI control scheme.

2.5 Optimization of DH systems

The optimal set point strategy is very useful for energy savings in DH systems. A number of studies have been done on this subject.

Zheng Guorong (1997) [27] developed dynamic models and optimal control for a multi-zone HVAC systems. A methodology was developed to determine the optimal set point profiles based on dynamic characteristics of the overall system. The results showed the potential to energy savings and improved comfort of the occupants under several operating conditions. A global optimal control methodology to handle multiple stage operation and multiple time scale processes was presented.

Wen Zhen Huang, Zaheer-uddin, Cho, (2005) [26] developed five energy management control functions for operation of HVAC systems. Based on a sequential quadratic programming method, a "medium-scale optimization" algorithm was used to find the optimal set point profiles during the predetermined ranges. The results showed that more than 17% energy was saved by using optimal set points compared to constant set point on the system.

Bojic, Trifunovic, Gustafsson, (2000) [18] presented an optimal strategy to improve thermal comfort in buildings in the presence of changes in system characteristics. A bottom-up approach and mixed 0-1 sequential linear programming were used to find optimal strategy of problem mitigation by the adjustment of hydraulic resistance of existing valves and retrofitting heat exchanger and additional pumps in branch loops. The results showed that significant improvement of thermal comfort in buildings could be obtained by using optimal strategy if the underlying cause for deterioration was due to change in hydraulic resistance in some branch loops. However, the influence of hydraulic resistance to system performance such as energy efficiency was not investigated.

2.6 Summary

From the literature review above, the following issues are identified:

1) Most literature studies involving district heating systems focus on the one or several components in the system such as boiler, heater, and zone but very few of them considered the overall system including pipe insulation, balance and control valves, circulating and makeup water pumps, etc.

2) Most studies on energy consumption of DH systems focus on thermal system. No detailed study of hydraulic system and its impact on energy consumption is done.
3) In most dynamic models of DH systems, all heat lost from pipe network to the ground and inter-pipe losses are ignored.
4) In the few studies involving combined dynamic thermal model and steady–state hydraulic model, the impact of the hydraulic parameters on the thermal model is not examined.
5) In the hydraulic models of DH system, how the balance valve influences the performance of network and energy efficiency of DH system is not studied.
6) There have been many studies involving control methods and operation strategies in DH system, but how these operations influence the hydraulic balancing and how to take advantage of balance valves in the system to improve energy efficiency is not studied.

2.7 Objectives of the thesis

The objectives of this thesis are to study the effects of balancing valve on energy efficiency of DH system and find optimal operation strategies for the system. The specific objectives are stated below.

1) Design a physical model of a DH system consisting of five residential and a commercial building.
2) Develop a dynamic model of a district heating system consisting of sub-system models such as boiler, supply and return water circuits, environmental zones, terminal radiators and exterior wall of building, etc. This dynamical model will be used to study the water and air temperatures response trend with time under different heat load conditions. The purpose is to find the relationship between outdoor air temperature and supply water temperature for this system.
3) Develop a hydraulic model of the district heating system to study water pressure distribution in DH system, water pressure drop on control and balancing valves, balancing valve performance evaluation and balancing valve opening position with the outdoor air temperature under different hydraulic conditions. The purpose is to find the relationship between balancing valves opening with outdoor air temperature which can be used to couple with the dynamics of the thermal system.
4) Design PI control strategies for boiler and zone control to keep supply water temperature and zone air temperatures close to set points in real operating conditions. Compare the system performance and energy efficiency with and without PI control under different conditions.
5) Optimize the control set points of DH system such as supply water temperature and

mass flow rate to improve the energy efficiency. The optimal balancing valve opening positions as a function of load will be identified to improve energy efficiency.

CHAPTER 3

Dynamic Model of DH system

3.1 Introduction

The dynamic model of a district heating system (DH system) is developed in this chapter. Since in DH system, the supply and return water temperature of each loop, zone air temperature of each building, are the most important parameters, the model will focus on calculating and analyzing those temperatures. First, the physical system will be designed. Then the dynamic model of each component, including boiler, supply and return water, zone air, enclosure structure and terminal heater will be built. Third, all of the component models will be integrated to build dynamic model of overall district heating system (DH system). Finally, open loop simulation results will be presented to study the dynamic responses of the district heating system (DH system).

3.2 Physical Model and Design of DH system

The schematic diagram of the DH system is shown in Figure 3.1. The DH system consists of a heat source, a water distribution system, and six terminal building user systems.

The main component of the heat source is the hot water boiler. It can supply required hot water by the whole system at a designed set point temperature. The capacity of the boiler is one of the most important factors in the design and selection process. At the

same time, the other parameters such as the maximum combustion efficiency should also be considered in this process.

The distribution system consists of supply water piping network and return water piping network, circulating water pumps, balance valves, and the makeup water system that maintains constant pressure at the return water pressure set point. The DH system transfers thermal energy from the boiler to different users by circulating hot water through the supply and return water piping network. The circulating water pumps must satisfy the water pressure required to transport the water from supply center to the farthest user. The balance valves will be necessary in different branch loops to ensure correct distribution of the water mass flow in the DH system. The makeup water system will keep up a constant initial water pressure to ensure the critical loop water supply and return and also replenish the water leaked in the piping network.

User systems include terminal heaters, control valves and indoor piping network. The supply water is circulated through the water piping network to each terminal heater thereby heating the space. The heater size and type will directly influence the efficiency of heat exchange.

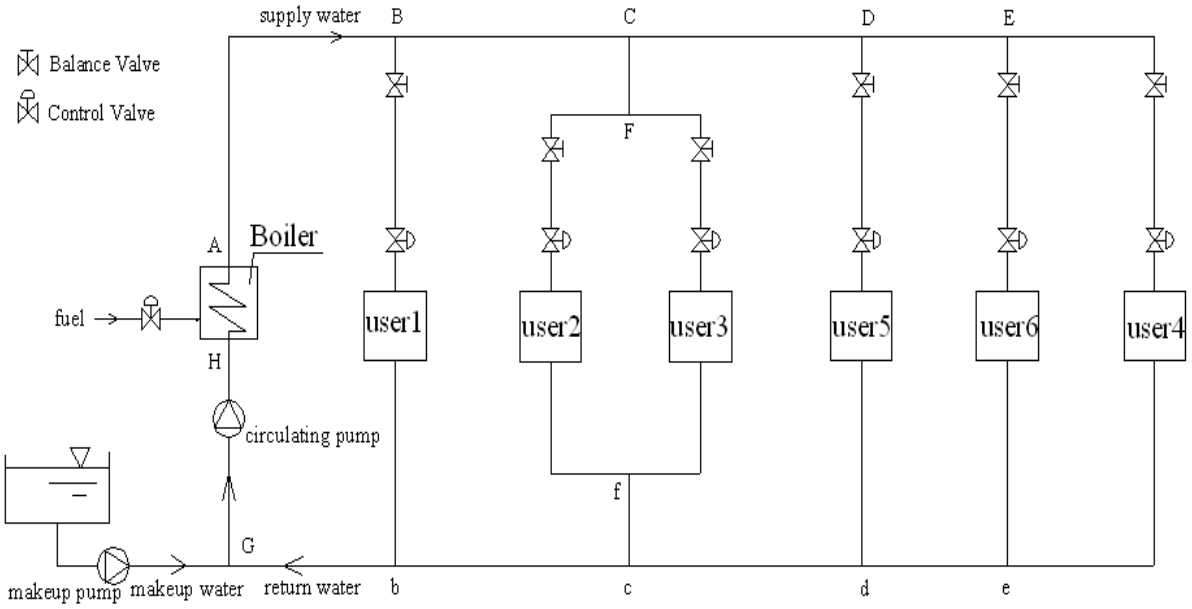

Figure 3.1 The schematic diagram of the DH system

3.2.1 Design Conditions

The designed heating system has 6 buildings with total heated floor area of 107600m^2 and total designed heating load of 5.35MW. The heated floor area of the two types of buildings namely commercial and residential buildings are 27300m^2 and 80300m^2 respectively. The average heat load rate per unit heated floor area is given in Table 3.1.

Building No.	1	2	3	4	5	6
Building Type	residential	residential	residential	residential	commercial	residential
Heated Floor Area A_{di} (m^2)	11500	22700	14800	20500	27300	10800
Heating load Index q_d (W/m^2)	51	46	47	45	56	53

Table 3.1 The average heating load index

Each building has 7 floors and the height of each floor is 2.4 m. In addition, the distribution system has five branches such as B-1, C-F-2(3), D-5, E-6, and E-4 as shown in Figure 3.1. All pipe lengths include the branch and the main pipes. Assume the length of the supply water loop and the return water loop is equal. The supply water temperature and return water temperature are 95 ℃ and 70 ℃ respectively. The outdoor design temperature is -15℃ and indoor design temperature is 18℃. Additional design parameters are given in Table 3.2.

Symbol	Item	Unit	Data
T_{sd}	Design supply water temperature	℃	95
T_{rd}	Design return water temperature	℃	70
T_{mk}	Makeup water temperature	℃	5
T_{zd}	Design indoor air temperature	℃	18
T_{od}	Design outdoor air temperature	℃	-15
c_w	Specific heat of water	J/Kg℃	4187
ρ_w	Water density (when T=75°C)	Kg/m^3	975
c_z	Specific heat of air	J/Kg℃	1000
HV	Heat value of the fuel	MJ/kg	43.35
T_{soil}	Average surface temperature of ground	℃	-2
ΔP_{bd}	Water resistance of boiler	kP_a	80
ΔP_{u1}	Water resistance of user 1	kP_a	30
ΔP_{u2}	Water resistance of user 2	kP_a	30
ΔP_{u3}	Water resistance of user 3	kP_a	30
ΔP_{u4}	Water resistance of user 4	kP_a	30
ΔP_{u5}	Water resistance of user 5	kP_a	30
ΔP_{u6}	Water resistance of user 6	kP_a	30

Table 3.2 Design Parameters

3.2.2 Design Procedure

The design procedure is summarized in the following.

3.2.2.1 Heat Load Q_{di} of each building

Based on the given design area and heating load index, calculate the design heating load for each building as shown below:

$$Q_{di} = q_{di} A_{di} \tag{3.1}$$

The calculated designed heat loads Q_{di} of each building are $Q_{d1} = 586500\text{W}$, $Q_{d2} = 1044200\text{W}$, $Q_{d3} = 695600\text{W}$, $Q_{d4} = 922500\text{W}$, $Q_{d5} = 1528800\text{W}$, $Q_{d6} = 572400\text{W}$ respectively.

3.2.2.2 Designed water mass flow rate

The designed circulating water mass flow rate G_{di} for each building is calculated as below:

$$G_{di} = \frac{Q_{di}}{c_w (T_{sd} - T_{rd})} \tag{3.2}$$

Where the water specific heat $c_w = 4187$ J/kg℃

The designed circulating water mass flow rate G_{di} of various buildings are G_{d1} = 5.60kg/s, $G_{d2} = 9.98$kg/s, $G_{d3} = 6.65$kg/s, $G_{d4} = 8.81$kg/s, $G_{d5} = 14.61$kg/s, $G_{d6} = 5.47$kg/s respectively.

3.2.2.3 The adjusted circulating water flow rate G_{ci}

Considering the heat loss during the transmission of hot water from the boiler to terminal heater in the piping network, the adjusted circulating water flow rate G_{ci} can be calculated as below:

$$G_{ci} = f_g G_{di} \tag{3.3}$$

Here f_g is the safety factor; the values range typically from 1.07 to 1.25.

With the safety factor f_g of 1.12, the adjusted water flow rate G_{ci} of various buildings are $G_{c1} = 6.28$kg/s, $G_{c2} = 11.17$kg/s, $G_{c3} = 7.44$kg/s, $G_{c4} = 9.87$kg/s, $G_{c5} = 16.36$kg/s, $G_{c6} = 6.12$ kg/s.

The circulating water flow rates for all buildings are summarized in Table 3.3.

user	A_{di}(m^2)	U_{di}(w/m^2)	q_d (w)	G_d (t/h)	G_c (t/h)	G_d (kg/s)	G_c (kg/s)
1	11500	51	586500	20.18	22.60	5.60	6.28
2	22700	46	1044200	35.92	40.23	9.98	11.17
3	14800	47	695600	23.93	26.80	6.65	7.44
4	20500	45	922500	31.73	35.54	8.81	9.87
5	27300	56	1528800	52.59	58.90	14.61	16.36
6	10800	53	572400	19.69	22.05	5.47	6.12
Total	107600		5350000	184.04	206.12	51.11	57.24

Table 3.3 Buildings circulating water flow rate

3.2.2.4 Pipe sizes and hydraulic calculations

- Choose water flow velocity V in the range of 0.5m/s～1.5m/s, In this case, choose $V = 1.0$ m/s and calculate the pipe diameter.

- Calculate water flow rate of each pipe segment

  Based on the water flow rates of each building calculated previously G_c, the water flow rates G_{cp} in all pipe segments can be calculated by mass conservation equations. The calculated results for each pipe segment are shown in Table 3.4.

- Determine each pipe segment diameter d_{cp}

  With the water flow rate G_{cp} and velocity V, the pipe diameter can be calculated by the formula as below:

$$d_{cp} = 2\sqrt{\frac{G_{cp}}{\pi \rho V}} \tag{3.4}$$

  Where the water density $\rho = 961.92 \text{kg/m}^3$, at water temperature $T_w = 95℃$

Based on the calculated pipe segment diameters, the normal pipe diameters d_p are selected as given in Table 3.4.

Pipe Segment	G_{cp}(kg/s)	d_{cp}(m)	d_p(m)	d_p(mm)	ϕ(mm)
AB	57.24	0.2753	0.2	200	ϕ219*6
BC	50.97	0.2598	0.2	200	ϕ219*6
CD	32.35	0.2070	0.2	200	ϕ219*6
DE	22.48	0.1455	0.15	150	ϕ159*4.5
B1	6.28	0.0911	0.07	70	ϕ76*3.5
CF	18.62	0.1570	0.15	150	ϕ159*4.5
F2	11.17	0.1216	0.125	125	ϕ133*4
F3	7.44	0.0993	0.125	125	ϕ133*4
E4	9.87	0.1143	0.15	150	ϕ159*4.5
D5	16.36	0.1472	0.15	150	ϕ159*4.5
E6	6.12	0.0900	0.1	100	ϕ108*4

Table 3.4 The pipe segment diameter

- Determine friction rate R_{cp} of each pipe segment

  The friction rate R_{cp} can be calculated by the formula as below:

$$R_{cp} = 6.25\times10^{-8}\times\frac{\lambda_{cp}G_{cp}^{\ 2}}{\rho d_{cp}^{\ 5}} = 6.875\times10^{-9}\times\frac{K^{0.25}G_{cp}^{\ 2}}{\rho d_{cp}^{\ 5.25}} \quad (3.5)$$

  Where friction factor $\lambda_{cp} = 0.11\left(\frac{K}{d_{cp}}\right)^{0.25}$,

  The equivalent absolute roughness K of hot water distribution system is assumed as 0.0005 m. With hot water density $\rho = 961.92\text{kg/m}^3$ at 95℃, the friction rates of pipe segments were calculated and are tabulated in Table 3.5.

LINE	V (m/s)	λ	R (Pa/m)	L_{cp} (m)	L_{dp} (m)	ΔP_i (Pa)
AB	1.69	0.0246	169.14	235	282	47698.66
BC	1.51	0.0246	134.09	95	114	15286.45
CD	0.96	0.0246	54.03	110	132	7131.83
DE	0.84	0.0264	59.80	80	96	5740.81
B1	1.51	0.0320	503.19	30	39	19624.24
CF	0.98	0.0264	81.00	50	65	5264.90
F2	0.85	0.0277	75.99	40	52	3951.39
F3	0.56	0.0277	33.72	175	227.5	7671.49
E4	0.52	0.0264	22.77	135	175.5	3996.57
D5	0.86	0.0264	62.54	120	156	9756.72
E6	0.72	0.0293	73.68	40	52	3831.42

Table 3.5 Friction drops of pipe segments

- Calculate the equivalent length L_{dp} of each pipe segment

$$L_{dp} = (1+\alpha)L_{cp} \tag{3.6}$$

Here the partial friction rate α of main pipe segments and branch pipe segments are selected as 0.2 and 0.3 respectively. For details please see table 3.5.

- Calculate the friction resistance ΔP_i of each circuit loop

$$\Delta P_i = \sum \Delta P_{ip} + \Delta P_b + \Delta P_u + \Delta P_v \tag{3.7}$$

$$\Delta P_{ip} = L_{dp} R_{cp} \tag{3.8}$$

Where ΔP_b = the friction resistance of boiler, Pa

ΔP_u = The friction resistance of building, Pa

ΔP_v = The friction resistance of control valve, Pa

ΔP_{ip} = The friction resistance of pipe segment, Pa

The friction resistances of all six loops are shown in table 3.6.

loop	$\sum \Delta P_{ip}$ (Pa)	ΔP_b (Pa)	ΔP_u (Pa)	ΔP_{cv} (Pa)	ΔP_i (Pa)	ΔP_{bv} (Pa)
1	134645.82	80000	30000	30000	274645.82	25101.51
2	144402.81	80000	30000	30000	284402.81	15344.52
3	151843.02	80000	30000	30000	291843.02	7904.31
4	159708.66	80000	30000	30000	299708.66	38.67
5	159378.35	80000	30000	30000	299378.35	368.98
6	159747.33	80000	30000	30000	299747.33	0.00

Table 3.6 Friction resistance of each loop

3.2.2.5 Select circulating pump

The circulating pump capacity can be determined as below

$$G_p = f_f G_c \tag{3.9}$$

Where the circulating water flow rate $G_c = \sum G_{ci}$

The safety factor of circulating water flow rate f_f typically follows the range from 1.05 to 1.15.

With the safety factor $f_f = 1.1$, the water flow rate G_p of circulating pump is 62.97kg/s.

With the largest resistance of the circuit loop 6 in this system (Figure 3.1), determine the pressure head of the circulating pump using the formula given below:

$$\Delta P_p = f_r \Delta P_i \tag{3.10}$$

Here the safety factor of water friction resistance f_r is considered. The value typically falls in the range from 1.1 to 1.2.

With a safety factor $f_r = 1.15$, the pressure head of the circulating pump is 344709Pa.

3.2.2.6 Boiler capacity

Determine the thermal capacity of the boiler as below:

$$Q = f_g \sum_{i=1}^{n} q_{di} \tag{3.11}$$

With the safety factor f_g of 1.1, the calculated capacity of the boiler is 5885000W.

Here a gas boiler with 7MW thermal capacity was chosen. The other parameters include the volume V=6m^3, hot water capacity $m_{bd} = 200$ t/h, the maximum efficiency $\eta_{b\max} = 0.85$.

3.2.2.7 Makeup water pump

Determine the capacity of makeup water pump as below:

$$G_m = f_m G_p \tag{3.12}$$

With $G_p = 62.97$kg/s, the makeup water flow rate $G_m = 1.89$kg/s, assuming $f_m = 3\%$.

Determine the pressure head of makeup water pump as below:

$$\Delta P_m = f_{mp} P_m \tag{3.13}$$

Where the safety factor f_{mp} ranges between 1.05 to 1.2.

The makeup water pressure is related to several factors such as elevation of the buildings, position of the makeup water set point, highest permitted pressure of terminal heaters, the highest point of the whole system and the lowest permitted inlet pressure of circulating pumps.

With the safety factor $f_{mp} = 1.1$ and $P_m = 230000$Pa, the makeup water pressure set point $\Delta P_m = 253000$Pa.

3.2.2.8 Balancing valves

Determine the balance valve setting as below:

$$\Delta P_{bvi} = \Delta P_{i\max} - \Delta P_i \tag{3.14}$$

Based on industry experience, it is generally accepted that the difference of water resistance between the largest resistance loop and other loops should be less than 10%. Otherwise, either adjusting the pipe dimension again or the use of throttling device is recommended.

The largest friction resistance loop is 6, which has the friction resistance of 299747Pa. The smallest friction resistance loop is 1, which has the friction resistance of 274645Pa. The percentage difference R_d of friction resistances in each loop shown in table 3.7

Based on the difference in the friction resistance of each loop under the design condition, the pressure drops of different balance valves are shown in table 3.7.

loop	$\sum \Delta P_{ip}$ (Pa)	ΔP_i (Pa)	R_d (%)	ΔP_{bv} (Pa)
1	134645.82	274645.82	8.37%	25101.51
2	144402.81	284402.81	5.12%	15344.52
3	151843.02	291843.02	2.64%	7904.31
4	159708.66	299708.66	0.01%	38.67
5	159378.35	299378.35	0.12%	368.98
6	159747.33	299747.33	0.00%	0.00

Table 3.7 Pressure balance on each loop

3.2.3 Design parameters

The design procedure described above was used to develop a design program. The results obtained along with some important design parameters of DH system are listed in table 3.8.

Symbol	Item	Unit	Data
A_{di}	Heated floor area	m^2	107600
q_{di}	Heating load	MW	5.35
G_d	Design circulating water flow rate	t/h	184.04
V_b	volume of the boiler	m^3	6
f_m	Ratio of makeup water	%	3
$\eta_{b\max}$	Maximum efficiency of the boiler	%	85
Q_{bd}	Thermal capacity of boiler	MW	7
m_{bd}	Hot water capacity of boiler	t/h	200

Table 3.8 Design parameters of DH system

3.3 Dynamic Model of DH system

In the following dynamic models of sub-systems are developed using energy balance principles.

3.3.1 Boiler model

An accurate dynamic model of a boiler is very complex. To simplify the dynamic model of the boiler, some operating data from practice is used, such as the efficiency and temperature relationship curve. Five data points of efficiency versus boiler temperature from the curve were taken. These are

$e_b = [0.55, 0.68, 0.77, 0.83, 0.85]$ With $T_b = [50, 60, 70, 80, 90]$

A polynomial equation corresponding to this data set was obtained. The resulting equation is $e_b = -0.0002T_b^2 + 0.0325T_b - 0.6283$,

The boiler model is developed in which the rate of heat stored in the supply water is equated to the heat produced by boiler minus the heat lost by the makeup water.

$$C_b \frac{d(T_b)}{dt} = u_f m_{f\max} e_b HV - c_w(m_{dtot} + 0.5G_{mk})(T_b - T_r) \quad (3.15)$$

Where $C_b =$ Thermal capacity of boiler, $J/°C$ ($C_b = \rho c_w V_b$)

$T_b =$ The output water temperature from boiler, ℃

$u_f =$ Fuel flow rate control variable

$m_{f\max}$ = The maximum mass flow rate of fuel, kg/s

e_b = The boiler efficiency,

HV = The heating value of fuel, J/kg

c_w = The specific heat of water, $J/kg°C$

m_{dtot} = The design total supply water flow rate, kg/s

G_{mk} = The flow rate of makeup water, kg/s

T_r = The return water temperature, ℃

3.3.2 Supply and return water temperatures model

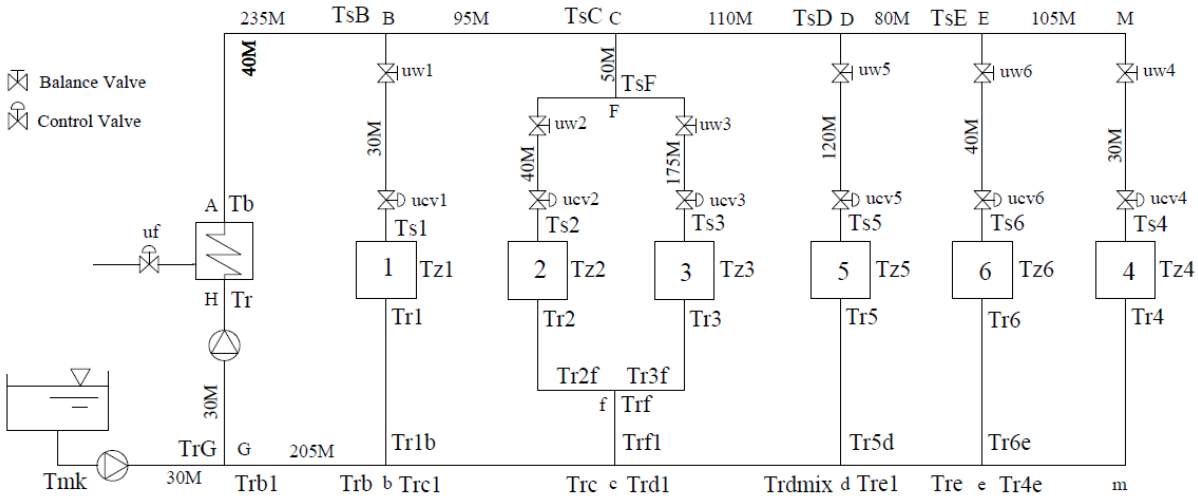

Figure 3.2 The schematic diagram of the supply and return water temperatures model

In a district heating system, the heat source is always farther to buildings than the other types of heating systems. As such the factors causing heat loss in the network are also more than in the other systems, and to this end, the temperature changes occurring in different pipe segments should be simulated to compute heat losses through the pipes.

The supply and return water pipes shown in Figure 3.2 were divided into twenty-nine segments, so there are a total of twenty-nine temperature nodes in this system. Heat balance equations will be used to describe the dynamics of these nodes.

For each node, the heat stored equals the heat supplied by adjacent segment minus the heat lost by the pipe wall and the water leakage.

For supply water network we have the following equations:

$$C_{AB}\frac{d(T_{sB})}{dt} = c_w m_{AB}(T_b - T_{sB}) - Q_{lsAB} - c_w m_{ABmk}(0.5(T_b + T_{sB}) - T_{mk}) \tag{3.16}$$

$$C_{BC}\frac{d(T_{sC})}{dt} = c_w m_{BC}(T_{sB} - T_{sC}) - Q_{lsBC} - c_w m_{BCmk}(0.5(T_{sB} + T_{sC}) - T_{mk}) \tag{3.17}$$

$$C_{CD}\frac{d(T_{sD})}{dt} = c_w m_{CD}(T_{sC} - T_{sD}) - Q_{lsCD} - c_w m_{CDmk}(0.5(T_{sD} + T_{sC}) - T_{mk}) \tag{3.18}$$

$$C_{DE}\frac{d(T_{sE})}{dt} = c_w m_{DE}(T_{sD} - T_{sE}) - Q_{lsDE} - c_w m_{DEmk}(0.5(T_{sD} + T_{sE}) - T_{mk}) \tag{3.19}$$

$$C_{s4}\frac{d(T_{s4})}{dt} = c_w m_{E4}(T_{sE} - T_{s4}) - Q_{lsE4} - c_w m_{E4mk}(0.5(T_{s4} + T_{sE}) - T_{mk}) \tag{3.20}$$

$$C_{sF}\frac{d(T_{sF})}{dt} = c_w m_{CF}(T_{sC} - T_{sF}) - Q_{lsCF} - c_w m_{CFmk}(0.5(T_{sC} + T_{sF}) - T_{mk}) \tag{3.21}$$

$$C_{B1}\frac{d(T_{s1})}{dt}=c_w m_{B1}(T_{sB}-T_{s1})-Q_{lsB1}-c_w m_{B1mk}(0.5(T_{sB}+T_{s1})-T_{mk}) \quad (3.22)$$

$$C_{F2}\frac{d(T_{s2})}{dt}=c_w m_{F2}(T_{sF}-T_{s2})-Q_{lsF2}-c_w m_{F2mk}(0.5(T_{sF}+T_{s2})-T_{mk}) \quad (3.23)$$

$$C_{F3}\frac{d(T_{s3})}{dt}=c_w m_{F3}(T_{sF}-T_{s3})-Q_{lsF3}-c_w m_{F3mk}(0.5(T_{sF}+T_{s3})-T_{mk}) \quad (3.24)$$

$$C_{D5}\frac{d(T_{s5})}{dt}=c_w m_{D5}(T_{sD}-T_{s5})-Q_{lsD5}-c_w m_{D5mk}(0.5(T_{sD}+T_{s5})-T_{mk}) \quad (3.25)$$

$$C_{E6}\frac{d(T_{s6})}{dt}=c_w m_{E6}(T_{sE}-T_{s6})-Q_{lsE6}-c_w m_{E6mk}(0.5(T_{sE}+T_{s6})-T_{mk}) \quad (3.26)$$

For the return water network, the energy balance equations are

$$C_{htr1}\frac{d(T_{r1})}{dt}=c_w m_{B1}(T_{s1}-T_{r1})-U_{htr1}[0.5(T_{s1}+T_{r1})-T_{z1}]^{(1+c_1)} \quad (3.27)$$

$$C_{htr2}\frac{d(T_{r2})}{dt}=c_w m_{F2}(T_{s2}-T_{r2})-U_{htr2}[0.5(T_{s2}+T_{r2})-T_{z2}]^{(1+c_2)} \quad (3.28)$$

$$C_{htr3}\frac{d(T_{r3})}{dt}=c_w m_{F3}(T_{s3}-T_{r3})-U_{htr3}[0.5(T_{s3}+T_{r3})-T_{z3}]^{(1+c_3)} \quad (3.29)$$

$$C_{htr5}\frac{d(T_{r5})}{dt}=c_w m_{D5}(T_{s5}-T_{r5})-U_{htr5}[0.5(T_{s5}+T_{r5})-T_{z5}]^{(1+c_5)} \quad (3.30)$$

$$C_{htr6}\frac{d(T_{r6})}{dt}=c_w m_{E6}(T_{s6}-T_{r6})-U_{htr6}[0.5(T_{s6}+T_{r6})-T_{z6}]^{(1+c_6)} \quad (3.31)$$

$$C_{htr4}\frac{d(T_{r4})}{dt}=c_w m_{E4}(T_{s4}-T_{r4})-U_{htr4}[0.5(T_{s4}+T_{r4})-T_{z4}]^{(1+c_4)} \quad (3.32)$$

Where $C_{htr1\sim6}$ = Thermal capacity of heaters 1~6, J/℃

$U_{htr1\sim6}$ = Actual heat transfer coefficient of heaters 1~6, W/℃

$c_{1\sim6}$ = The modified index for heat transfer coefficient.

$$C_{2f}\frac{d(T_{r2f})}{dt}=c_w m_{2f}(T_{r2}-T_{r2f})-Q_{ls2f}-c_w m_{2fmk}(0.5(T_{r2}+T_{r2f})-T_{mk}) \quad (3.33)$$

$$C_{3f}\frac{d(T_{r3f})}{dt}=c_w m_{3f}(T_{r3}-T_{r3f})-Q_{ls3f}-c_w m_{3fmk}(0.5(T_{r3}+T_{r3f})-T_{mk}) \quad (3.34)$$

$$C_{5d}\frac{d(T_{r5d})}{dt}=c_w m_{5d}(T_{r5}-T_{r5d})-Q_{ls5d}-c_w m_{5dmk}(0.5(T_{r5}+T_{r5d})-T_{mk}) \quad (3.35)$$

$$C_{6e}\frac{d(T_{r6e})}{dt}=c_w m_{6e}(T_{r6}-T_{r6e})-Q_{ls6e}-c_w m_{6emk}(0.5(T_{r6}+T_{r6e})-T_{mk}) \quad (3.36)$$

$$C_{4e}\frac{d(T_{r4e})}{dt}=c_w m_{4e}(T_{r4}-T_{r4e})-Q_{ls4e}-c_w m_{4emk}(0.5(T_{r4}+T_{r4e})-T_{mk}) \quad (3.37)$$

$$C_{de}\frac{d(T_{re1})}{dt}=c_w m_{de}(T_{re}-T_{re1})-Q_{lsde}-c_w m_{demk}(0.5(T_{re}+T_{re1})-T_{mk}) \quad (3.38)$$

$$C_{cd}\frac{d(T_{rd1})}{dt}=c_w m_{cd}(T_{rd}-T_{rd1})-Q_{lscd}-c_w m_{d1mk}(0.5(T_{rd}+T_{rd1})-T_{mk}) \quad (3.39)$$

$$C_{fc}\frac{d(T_{rf1})}{dt}=c_w m_{fc}(T_{rf}-T_{rf1})-Q_{lsfc}-c_w m_{fcmk}(0.5(T_{rf}+T_{rf1})-T_{mk}) \quad (3.40)$$

$$C_{bc}\frac{d(T_{rc1})}{dt}=c_w m_{bc}(T_{rc}-T_{rc1})-Q_{lsbc}-c_w m_{bcmk}(0.5(T_{rc}+T_{rc1})-T_{mk}) \quad (3.41)$$

$$C_{1b}\frac{d(T_{r1b})}{dt}=c_w m_{1b}(T_{r1}-T_{r1b})-Q_{ls1b}-c_w m_{1bmk}(0.5(T_{r1}+T_{r1b})-T_{mk}) \quad (3.42)$$

$$C_{bG}\frac{d(T_{rb1})}{dt}=c_w m_{bG}(T_{rb}-T_{rb1})-Q_{lsbG}-c_w m_{bGmk}(0.5(T_{rb}+T_{rb1})-T_{mk}) \quad (3.43)$$

$$C_{gh}\frac{d(T_r)}{dt}=c_w m_{gh}(T_{rG}-T_r)-Q_{lsgh}-c_w m_{ghmk}(0.5(T_{rG}+T_r)-T_{mk}) \quad (3.44)$$

The mixed water temperatures T_{rf}, T_{re}, T_{rd}, T_{rc}, T_{rb}, T_{rG} of return water are described as below:

$$T_{rf} = (T_{r2f} u_{w2} m_{2d} + T_{r3f} u_{w3} m_{3d}) / (u_{w2} m_{2d} + u_{w3} m_{3d}) \tag{3.45}$$

$$T_{re} = (T_{r4e} u_{w4} m_{4d} + T_{r6e} u_{w6} m_{6d}) / (u_{w4} m_{4d} + u_{w6} m_{6d}) \tag{3.46}$$

$$T_{rdmix} = (T_{r5d} u_{w5} m_{5d} + T_{re1}(u_{w6} m_{6d} + u_{w4} m_{4d})) / (u_{w5} m_{5d} + u_{w6} m_{6d} + u_{w4} m_{4d}) \tag{3.47}$$

$$T_{rc} = (T_{rf1}(u_{w2} m_{2d} + u_{w3} m_{3d}) + T_{rd1}(u_{w5} m_{5d} + u_{w6} m_{6d} + u_{w4} m_{4d})) / (u_{w2} m_{2d} + u_{w3} m_{3d} + u_{w5} m_{5d} + u_{w6} m_{6d} + u_{w4} m_{4d}) \tag{3.48}$$

$$T_{rb} = (T_{r1b} u_{w1} m_{1d} + T_{rc1}(u_{w2} m_{2d} + u_{w3} m_{3d} + u_{w5} m_{5d} + u_{w6} m_{6d} + u_{w4} m_{4d})) / (u_{w1} m_{1d} + u_{w2} m_{2d} + u_{w3} m_{3d} + u_{w5} m_{5d} + u_{w6} m_{6d} + u_{w4} m_{4d}) \tag{3.49}$$

$$T_{rG} = (T_{mk} G_{mk} + T_{rb1}(u_{w1} m_{1d} + u_{w2} m_{2d} + u_{w3} m_{3d} + u_{w5} m_{5d} + u_{w6} m_{6d} + u_{w4} m_{4d})) / (u_{w1} m_{1d} + u_{w2} m_{2d} + u_{w3} m_{3d} + u_{w5} m_{5d} + u_{w6} m_{6d} + u_{w4} m_{4d} + G_{mk}) \tag{3.50}$$

Where T_{mk} = The makeup water temperature, ℃

Q_{lsi} = The heat lost from pipe segment i, W

Due to the fact that the supply and return water pipes are parallel and embedded underground, the additional heat transfer between supply and return pipe segments should be considered. The equations describing this interaction are shown below:

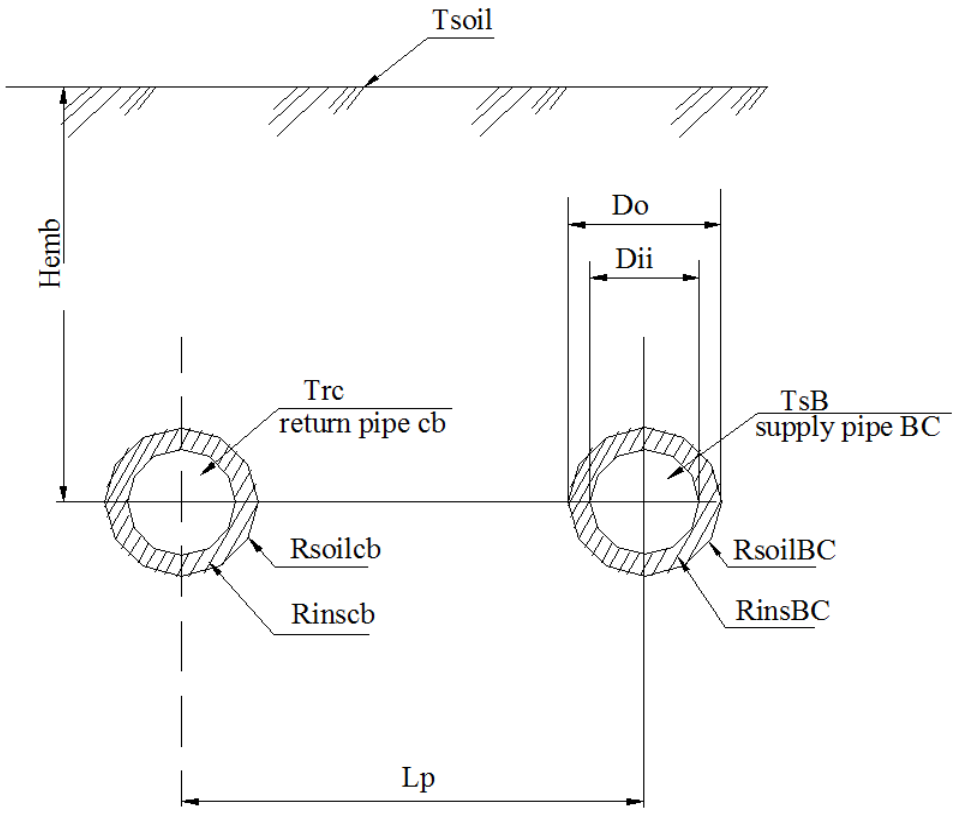

Figure 3.3 The schematic diagram of the supply and return water pipe (segment BC and cb) under ground

$$Q_{lsAB} = [\frac{(T_b - T_{soil})(R_{insAB} + R_{soilAB}) - (T_{rb} - T_{soil})R_{\text{int}}}{(R_{insAB} + R_{soilAB})^2 - R_{\text{int}}^{\ 2}}](1+\beta)L_{AB} \tag{3.51}$$

$$Q_{lsBC} = [\frac{(T_{sB} - T_{soil})(R_{insBC} + R_{soilBC}) - (T_{rc} - T_{soil})R_{\text{int}}}{(R_{insBC} + R_{soilBC})^2 - R_{\text{int}}^{\ 2}}](1+\beta)L_{BC} \tag{3.52}$$

$$Q_{lsCD} = [\frac{(T_{sC} - T_{soil})(R_{insCD} + R_{soilCD}) - (T_{rdmix} - T_{soil})R_{\text{int}}}{(R_{insCD} + R_{soilCD})^2 - R_{\text{int}}^{\ 2}}](1+\beta)L_{CD} \tag{3.53}$$

$$Q_{lsDE} = [\frac{(T_{sD} - T_{soil})(R_{insDE} + R_{soilDE}) - (T_{re} - T_{soil})R_{\text{int}}}{(R_{insDE} + R_{soilDE})^2 - R_{\text{int}}^{\ 2}}](1+\beta)L_{DE} \tag{3.54}$$

$$Q_{lsCF} = [\frac{(T_{sC} - T_{soil})(R_{insCF} + R_{soilCF}) - (T_{rf} - T_{soil})R_{\text{int}}}{(R_{insCF} + R_{soilCF})^2 - R_{\text{int}}^{\ 2}}](1+\beta)L_{CF} \tag{3.55}$$

$$Q_{lsB1} = [\frac{(T_{sB} - T_{soil})(R_{insB1} + R_{soilB1}) - (T_{r1} - T_{soil})R_{\text{int}}}{(R_{insB1} + R_{soilB1})^2 - R_{\text{int}}^2}](1+\beta)L_{B1} \quad (3.56)$$

$$Q_{lsF2} = [\frac{(T_{sF} - T_{soil})(R_{insF2} + R_{soilF2}) - (T_{r2} - T_{soil})R_{\text{int}}}{(R_{insF2} + R_{soilF2})^2 - R_{\text{int}}^2}](1+\beta)L_{F2} \quad (3.57)$$

$$Q_{lsF3} = [\frac{(T_{sF} - T_{soil})(R_{insF3} + R_{soilF3}) - (T_{r3} - T_{soil})R_{\text{int}}}{(R_{insF3} + R_{soilF3})^2 - R_{\text{int}}^2}](1+\beta)L_{F3} \quad (3.58)$$

$$Q_{lsD5} = [\frac{(T_{sD} - T_{soil})(R_{insD5} + R_{soilD5}) - (T_{r5} - T_{soil})R_{\text{int}}}{(R_{insD5} + R_{soilD5})^2 - R_{\text{int}}^2}](1+\beta)L_{D5} \quad (3.59)$$

$$Q_{lsE6} = [\frac{(T_{sE} - T_{soil})(R_{insE6} + R_{soilE6}) - (T_{r6} - T_{soil})R_{\text{int}}}{(R_{insE6} + R_{soilE6})^2 - R_{\text{int}}^2}](1+\beta)L_{E6} \quad (3.60)$$

$$Q_{lsE4} = [\frac{(T_{sE} - T_{soil})(R_{insE4} + R_{soilE4}) - (T_{r4} - T_{soil})R_{\text{int}}}{(R_{insE4} + R_{soilE4})^2 - R_{\text{int}}^2}](1+\beta)L_{E4} \quad (3.61)$$

$$Q_{ls2f} = [\frac{(T_{r2} - T_{soil})(R_{ins2f} + R_{soil2f}) - (T_{sF} - T_{soil})R_{\text{int}}}{(R_{ins2f} + R_{soil2f})^2 - R_{\text{int}}^2}](1+\beta)L_{2f} \quad (3.62)$$

$$Q_{ls3f} = [\frac{(T_{r3} - T_{soil})(R_{ins3f} + R_{soil3f}) - (T_{sF} - T_{soil})R_{\text{int}}}{(R_{ins3f} + R_{soil3f})^2 - R_{\text{int}}^2}](1+\beta)L_{3f} \quad (3.63)$$

$$Q_{ls4e} = [\frac{(T_{r4} - T_{soil})(R_{ins4e} + R_{soil4e}) - (T_{sE} - T_{soil})R_{\text{int}}}{(R_{ins4e} + R_{soil4e})^2 - R_{\text{int}}^2}](1+\beta)L_{4e} \quad (3.64)$$

$$Q_{ls6e} = [\frac{(T_{r6} - T_{soil})(R_{ins6e} + R_{soil6e}) - (T_{sE} - T_{soil})R_{\text{int}}}{(R_{ins6e} + R_{soil6e})^2 - R_{\text{int}}^2}](1+\beta)L_{6e} \quad (3.65)$$

$$Q_{lsed} = [\frac{(T_{re} - T_{soil})(R_{insed} + R_{soiled}) - (T_{sD} - T_{soil})R_{\text{int}}}{(R_{insed} + R_{soiled})^2 - R_{\text{int}}^2}](1+\beta)L_{ed} \quad (3.66)$$

$$Q_{ls5d} = [\frac{(T_{r5} - T_{soil})(R_{ins5d} + R_{soil5d}) - (T_{sD} - T_{soil})R_{\text{int}}}{(R_{ins5d} + R_{soil5d})^2 - R_{\text{int}}^2}](1+\beta)L_{5d} \quad (3.67)$$

$$Q_{lsdc} = [\frac{(T_{rdmix} - T_{soil})(R_{insdc} + R_{soildc}) - (T_{sC} - T_{soil})R_{\text{int}}}{(R_{insdc} + R_{soildc})^2 - R_{\text{int}}^2}](1+\beta)L_{dc} \quad (3.68)$$

$$Q_{lsfc} = [\frac{(T_{rf} - T_{soil})(R_{insfc} + R_{soilfc}) - (T_{sC} - T_{soil})R_{\text{int}}}{(R_{insfc} + R_{soilfc})^2 - R_{\text{int}}^2}](1+\beta)L_{fc} \quad (3.69)$$

$$Q_{lscb} = [\frac{(T_{rc} - T_{soil})(R_{inscb} + R_{soilcb}) - (T_{sB} - T_{soil})R_{\text{int}}}{(R_{inscb} + R_{soilcb})^2 - R_{\text{int}}^2}](1+\beta)L_{cb} \quad (3.70)$$

$$Q_{ls1b} = [\frac{(T_{r1} - T_{soil})(R_{ins1b} + R_{soil1b}) - (T_{sB} - T_{soil})R_{\text{int}}}{(R_{ins1b} + R_{soil1b})^2 - R_{\text{int}}^2}](1+\beta)L_{1b} \quad (3.71)$$

$$Q_{lsbg} = [\frac{(T_{rb} - T_{soil})(R_{insbg} + R_{soilbg}) - (T_b - T_{soil})R_{\text{int}}}{(R_{insbg} + R_{soilbg})^2 - R_{\text{int}}^{\ 2}}](1+\beta)L_{bg} \quad (3.72)$$

$$Q_{lsgh} = [\frac{(T_{rG} - T_{soil})(R_{insgh} + R_{soil\text{g}h}) - (T_b - T_{soil})R_{\text{int}}}{(R_{insgh} + R_{soil\text{g}h})^2 - R_{\text{int}}^{\ 2}}](1+\beta)L_{gh} \quad (3.73)$$

Where

T_{soil} =average surface temperature of soil, ℃;

$R_{insi} = \frac{1}{2\pi k_{insp}} \ln \frac{D_o}{D_{ii}}$, the thermal resistance of insulation to pipe segment i, m·℃/W;

k_{insp} =thermal conductivity of pipe insulation, 0.033W/ m·℃,

D_o =outside diameter of pipe with insulation, m

D_{ii} =outside diameter of pipe without insulation, m

$R_{soili} = \frac{1}{2\pi k_{soil}} \ln \frac{4(H_{emb} + \frac{k_{soil}}{h_{soil}})}{D_o}$, Since $H_{emb} / D_o \geq 2$, the thermal resistance of soil to pipe segmenti , m·℃/W,

k_{soil} =conductivity of soil, 1.1W/ m·℃

H_{emb} =average height of embedded pipe, 1m

h_{soil} =heat transfer coefficient of air on the surface of the ground, 15W/ m^2·℃

D_o =outside diameter of pipe with insulation, m

$R_{\text{int}} = \frac{1}{2\pi k_{soil}} \ln \sqrt{\left[\frac{2(H_{emb} + \frac{k_{soil}}{h_{soil}})}{L_p}\right]^2} + 1$, the additional thermal resistance between supply and return pipe segment, m·℃/W,

L_p = average pitch between supply and return pipe, 0.6m

β = heat loss factor by fittings, 0.15

Note: Compared to the thermal resistances of insulation and soil, the inside surfaces resistance and the pipe wall thickness resistances are too small and therefore are neglected in the actual calculation.

3.3.3 Zone model

For this DH system, the six buildings are simulated as six independent zones, T_{z1}, T_{z2}, T_{z3}, T_{z4}, T_{z5}, T_{z6}. Heat lost by the exterior walls, windows, ceilings, floors and air exchanges of buildings and heat gain from the terminal heaters, solar radiation from the windows, solar energy absorbed by the walls and roofs and the internal heat resource due to occupancy will be considered in this model.

The resulting energy balance equations are shown as below:

$$C_{z1}\frac{d(T_{z1})}{dt} = c_w u_{w1} m_{1d}(T_{s1} - T_{r1}) + Q_{gain1} - U_{en1}(T_{z1} - T_o) \tag{3.74}$$

$$C_{z2}\frac{d(T_{z2})}{dt} = c_w u_{w2} m_{2d}(T_{s2} - T_{r2}) + Q_{gain2} - U_{en2}(T_{z2} - T_o) \tag{3.75}$$

$$C_{z3}\frac{d(T_{z3})}{dt} = c_w u_{w3} m_{3d}(T_{s3} - T_{r3}) + Q_{gain3} - U_{en3}(T_{z3} - T_o) \tag{3.76}$$

$$C_{z5}\frac{d(T_{z5})}{dt}=c_w u_{w5} m_{5d}(T_{s5}-T_{r5})+Q_{gain5}-U_{en5}(T_{z5}-T_o) \tag{3.77}$$

$$C_{z6}\frac{d(T_{z6})}{dt}=c_w u_{w6} m_{6d}(T_{s6}-T_{r6})+Q_{gain6}-U_{en6}(T_{z6}-T_o) \tag{3.78}$$

$$C_{z4}\frac{d(T_{z4})}{dt}=c_w u_{w4} m_{4d}(T_{s4}-T_{r4})+Q_{gain4}-U_{en4}(T_{z4}-T_o) \tag{3.79}$$

Where Q_{gain} =the zone heat gain from solar radiation and internal heat resources, W

U_{eni} =Overall heat transfer coefficient for each building enclosure, W/℃

3.3.4 Heater model

The terminal heater is an important equipment in the system because it directly influences the heat transfer efficiency from heating medium to zone air. So the actual heat transfer coefficient of heaters should be calculated.

The heat transfer coefficient of heater is a function of many factors. The equations are shown below:

$$U_{htr1}=f_1 Q_{1d}/[0.5(T_{s1}+T_{r1})-T_{zd}]^{(1+c_1)} \tag{3.80}$$

$$U_{htr2}=f_2 Q_{2d}/[0.5(T_{s2}+T_{r2})-T_{zd}]^{(1+c_2)} \tag{3.81}$$

$$U_{htr3}=f_3 Q_{3d}/[0.5(T_{s3}+T_{r3})-T_{zd}]^{(1+c_3)} \tag{3.82}$$

$$U_{htr4}=f_4 Q_{4d}/[0.5(T_{s4}+T_{r4})-T_{zd}]^{(1+c4)} \tag{3.83}$$

$$U_{htr5} = f_5 Q_{5d} / [0.5(T_{s5} + T_{r5}) - T_{zd}]^{(1+c5)} \quad (3.84)$$

$$U_{htr6} = f_6 Q_{6d} / [0.5(T_{s6} + T_{r6}) - T_{zd}]^{(1+c6)} \quad (3.85)$$

Where $U_{htr1\sim6}$ = actual heat transfer coefficient of heaters 1~6, W/℃

$f_{1\sim6}$ = The safety factor for heat transfer area of heater

c_i = The modified index for heat transfer coefficient of heater

3.3.5 Exterior wall model

The heat transfer through exterior walls of the building was modeled using energy balance approach. The exterior wall was divided into several nodes. Then the nodal equations were written.

In this thesis all exterior walls consisted of brick and insulation. The brick layer was divided in 3 nodes. In total four temperatures nodes were used for each wall. For six buildings a total of 96 nodal equations were used.

As an example for building 1, the nodal equations for four side walls are described in the following.

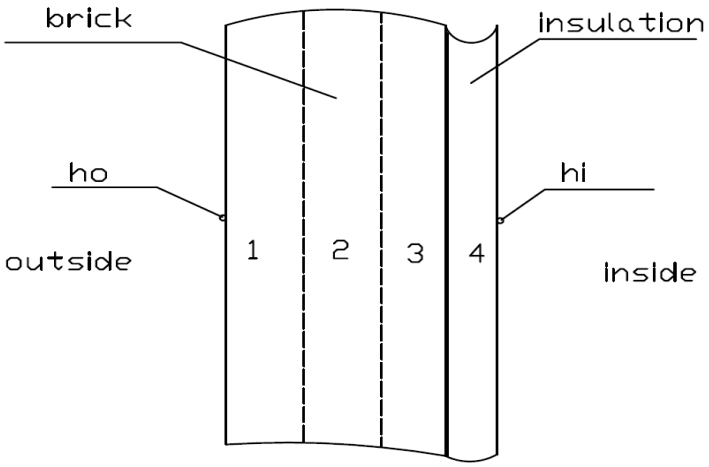

Figure 3.4 The exterior wall

South wall (building 1)

$$C_{1wls1}\frac{d(T_{1wls1})}{dt}=U_{1wlo1}A_{1wls}(T_o-T_{1wls1})+Q_{solwls1}+U_{1wl12}A_{1wls}(T_{1wls2}-T_{1wls1}) \tag{3.86}$$

$$C_{1wls2}\frac{d(T_{1wls2})}{dt}=U_{1wl12}A_{1wls}(T_{1wls1}-T_{1wls2})+U_{1wl23}A_{1wls}(T_{1wls3}-T_{1wls2}) \tag{3.87}$$

$$C_{1wls3}\frac{d(T_{1wls3})}{dt}=U_{1wl23}A_{1wls}(T_{1wls2}-T_{1wls3})+U_{1wl34}A_{1wls}(T_{1wls4}-T_{1wls3}) \tag{3.88}$$

$$C_{1wls4}\frac{d(T_{1wls4})}{dt}=U_{1wl34}A_{1wls}(T_{1wls3}-T_{1wls4})+U_{1wl4i}A_{1wls}(T_{Z1}-T_{1wls4}) \tag{3.89}$$

East wall (building 1)

$$C_{1wle1}\frac{d(T_{1wle1})}{dt}=U_{1wlo1}A_{1wle}(T_o-T_{1wle1})+Q_{solwle1}+U_{1wl12}A_{1wle}(T_{1wle2}-T_{1wle1}) \tag{3.90}$$

$$C_{1wle2}\frac{d(T_{1wle2})}{dt}=U_{1wl12}A_{1wle}(T_{1wle1}-T_{1wle2})+U_{1wl23}A_{1wle}(T_{1wle3}-T_{1wle2}) \quad (3.91)$$

$$C_{1wle3}\frac{d(T_{1wle3})}{dt}=U_{1wl23}A_{1wle}(T_{1wle2}-T_{1wle3})+U_{1wl34}A_{1wle}(T_{1wle4}-T_{1wle3}) \quad (3.92)$$

$$C_{1wle4}\frac{d(T_{1wle4})}{dt}=U_{1wl34}A_{1wle}(T_{1wle3}-T_{1wle4})+U_{1wl4i}A_{1wle}(T_{Z1}-T_{1wle4}) \quad (3.93)$$

West wall (building 1)

$$C_{1whw1}\frac{d(T_{1whw1})}{dt}=U_{1wlo1}A_{1whw}(T_o-T_{1whw1})+Q_{solwhw1}+U_{1wl12}A_{1whw}(T_{1whw2}-T_{1whw1}) \quad (3.94)$$

$$C_{1whw2}\frac{d(T_{1whw2})}{dt}=U_{1wl12}A_{1whw}(T_{1whw1}-T_{1whw2})+U_{1wl23}A_{1whw}(T_{1whw3}-T_{1whw2}) \quad (3.95)$$

$$C_{1whw3}\frac{d(T_{1whw3})}{dt}=U_{1wl23}A_{1whw}(T_{1whw2}-T_{1whw3})+U_{1wl34}A_{1whw}(T_{1whw4}-T_{1whw3}) \quad (3.96)$$

$$C_{1whw4}\frac{d(T_{1whw4})}{dt}=U_{1wl34}A_{1whw}(T_{1whw3}-T_{1whw4})+U_{1wl4i}A_{1whw}(T_{Z1}-T_{1whw4}) \quad (3.97)$$

North wall (building 1)

$$C_{1wln1}\frac{d(T_{1wln1})}{dt}=U_{1wlo1}A_{1wln}(T_o-T_{1wln1})+U_{1wl12}A_{1wln}(T_{1wln2}-T_{1wln1}) \quad (3.98)$$

$$C_{1wln2}\frac{d(T_{1wln2})}{dt}=U_{1wl12}A_{1wln}(T_{1wln1}-T_{1wln2})+U_{1wl23}A_{1wln}(T_{1wln3}-T_{1wln2}) \quad (3.99)$$

$$C_{1wln3}\frac{d(T_{1wln3})}{dt}=U_{1wl23}A_{1wln}(T_{1wln2}-T_{1wln3})+U_{1wl34}A_{1wln}(T_{1wln4}-T_{1wln3}) \quad (3.100)$$

$$C_{1w\ln 4}\frac{d(T_{1w\ln 4})}{dt}=U_{1wl34}A_{1w\ln}(T_{1w\ln 3}-T_{1w\ln 4})+U_{1wl4i}A_{1w\ln}(T_{Z1}-T_{1w\ln 4}) \quad (3.101)$$

Where $C_{1wl(s,e,w,n)(1,2,3,4)}=$thermal capacity of 1,2,3,4 layers on the south, east, west or north wall of building 1, J/℃

$U_{1wlo1},U_{1wl12},U_{1wl23},U_{1wl34},U_{1wl4i}=$overall heat-transfer coefficients of exterior wall nodes from the outside to inside of the building1, W/m$^2\cdot$℃

$Q_{solwl(s,e,w,)1}=$Heat gain from solar radiation from the south, east or west wall of building 1, W

3.4 Open loop responses of overall DH system

For the purpose of testing the validity of the developed overall DH system model, different operating conditions were chosen for open loop tests. The operating conditions include both design conditions and normal conditions. The design outdoor air temperature was set at -15°C during the testing period. All balance valves in the branch loops are kept at their initial balanced positions.

Based on different operating conditions, the outputs such as supply water temperature, return water temperature, room temperature and average room temperature response curves were plotted.

The input data for the open loop tests includes system design parameters, equipment characteristic curves and heat loss parameters. The results from open loop tests are discussed in the following.

3.4.1 System responses under design condition without internal heat gain

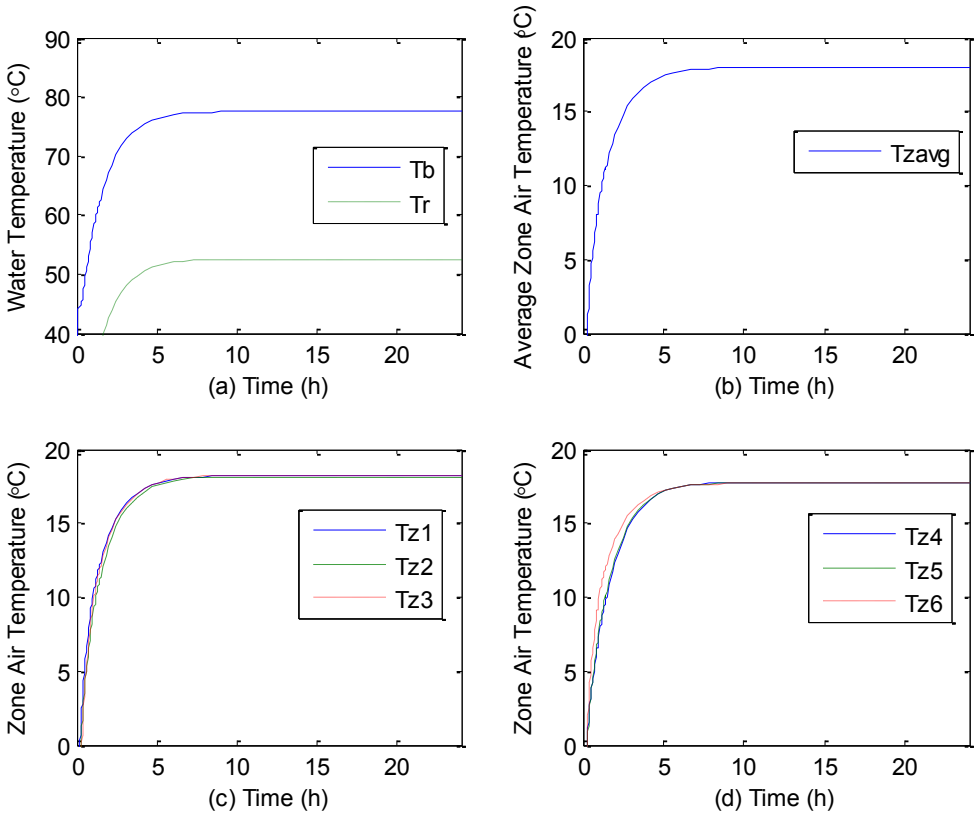

Figure 3.5 Temperatures response in design condition without internal heat gain

Figure 3.5, shows the temperature response under design condition. At the end of 24 hours, the temperatures of supply and return water reach 77.5 °C and 52.6 °C respectively, as well as the average air temperature in all zones is 18.0°C.

These temperatures reach steady state after about 10 hours. This delay reflects the amount of the thermal capacity of the system. Moreover, in the first 6 hours, the zone air temperatures have different responses because the capacity of each building is different.

The open loop responses shown in Figure 3.5 correspond to the following operating conditions.

The outside air temperature -15^{o}C is held constant, no heat gains from solar radiation and internal heat resources, no heat losses from pipe and no water leakage. Moreover all control valves were at full open position.

In order to keep the zone air temperatures at design set temperature at 18^{o}C, the fuel input control value was set at 0.768.

3.4.2 System responses under design condition without internal heat gain but with heat loss from pipes

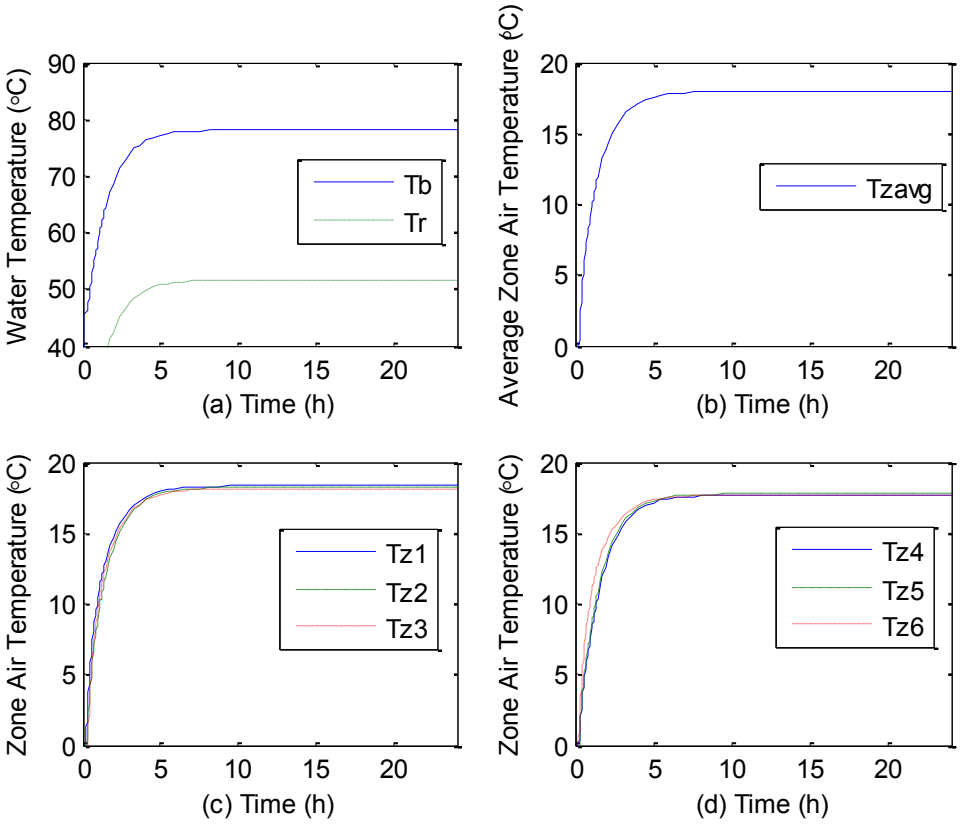

Figure 3.6 Temperatures response in design condition without heat gain but with heat loss from pipes

The temperatures responses for this case are depicted in Figure 3.6, under steady state, the temperatures of supply and return water reach78.1°C and 51.6°C respectively. In this case, the supply water temperature is higher and return water temperature is lower than the previous test (Figure 3.5) due to the heat loss from system.

The test conditions for this simulation remain the same as in the previous case (Figure 3.5) except for the additions of water leakage rate of 1.2%. The heat losses were also

included. The fuel input control to heat the zone to 18°C was found to be 0.813. This represents an increase in energy consumption to compensate for pipe losses from the system.

3.4.3 System responses under design condition with heat gains and pipe losses

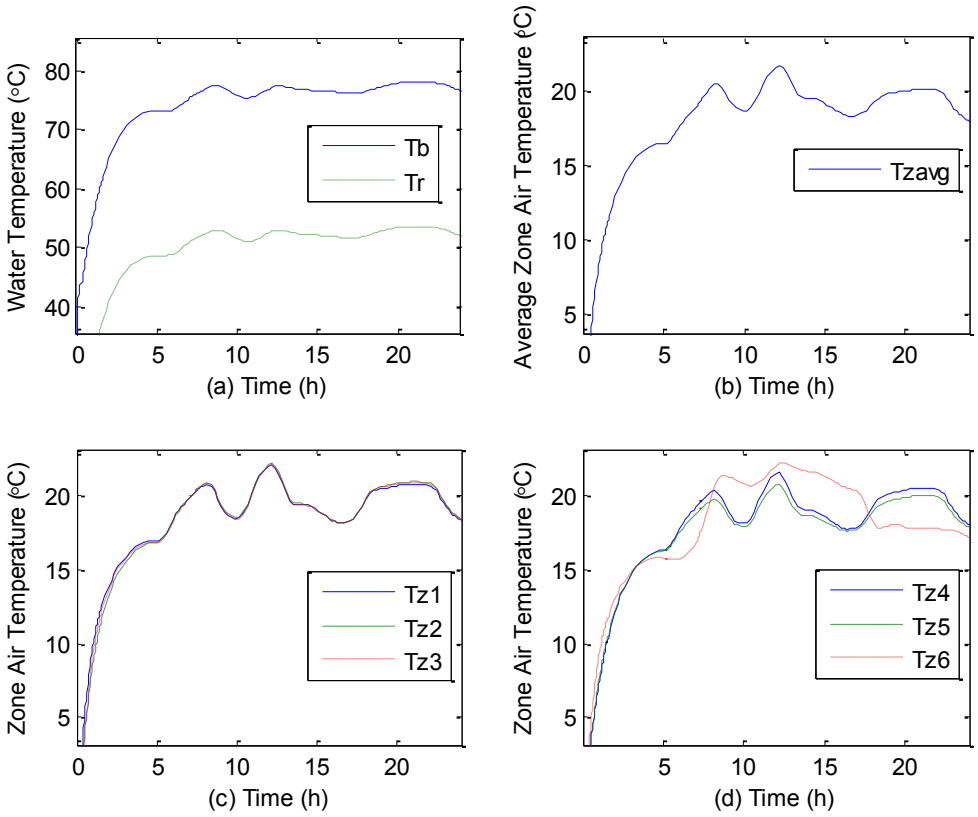

Figure 3.7 Temperatures response under design condition with heat gains and pipe losses

The temperatures responses for this case are depicted in Figure 3.7. Since the supply water mass flow rate and fuel input controls are constant in this condition, the temperatures obviously will change with the changes in heat load. In the Figure (d), the

zone 6 temperature trend is different from the other zones due to the effect of internal heat gain. The reason is that building 6 is a commercial building with significant internal heat gains and the other buildings are residential buildings.

3.4.4 Typical day responses with dynamic heat gains and pipe losses

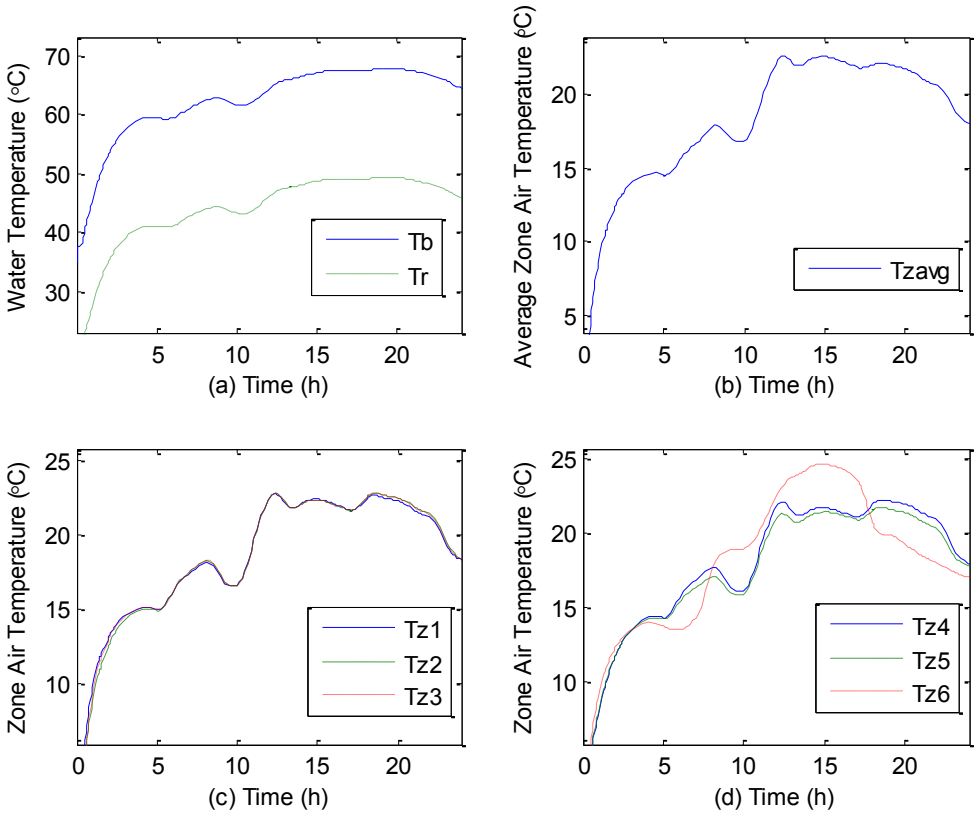

Figure 3.8 Temperatures response in normal condition with heat gains and pipe losses

A typical day responses with heat gains and pipe losses are depicted in Figure 3.8. Compared with Figure 3.7 the heat load changes caused by outdoor temperature will influence the temperature response trends. The range of zone air temperature changes in this figure is larger than that in Figure 3.6 due to the superimposed effect of outdoor temperature variations and internal heat gains.

The test conditions for this case are noted below:

The outside air temperature corresponds to a typical day data, the water leakage rate was 1.2%, heat gain from solar and internal heat resources were used to simulate a real building condition. The fuel input control was set at 0.619. In this case, all control valves were full open.

3.5 Summary

A physical model of DH system has been designed in this chapter. This model includes all main equipments like boiler, distribution pipe, control and balance valves, circulating and makeup water pumps and terminal heaters. A simplified design method for sizing the equipment has been presented.

Furthermore, a dynamic model of DH system has been developed. This model includes a boiler model, supply and return water temperature model, zone model, heater model and exterior wall model. These models can simulate the effect of load change such as outdoor temperature, solar radiation, internal heat gains and water leakage on the output responses of the system.

Open loop runs were made under different conditions with different input parameters. The resulting temperature responses are presented in this chapter.

This simulation model is useful to find relationship between outside air temperatures, the boiler supply water temperature; return water temperature and zone air temperature.

CHAPTER 4

Hydraulic Model of DH System

4.1 Introduction

A pipeline network for hot water transport and distribution from heat source to user is quite necessary in a DH system. The network performance is based on various hydraulic parameters such as water pressure, mass flow rate, pressure head of circulating pump, balance valve opening, etc. A model describing relationship among these parameters is required in order to build an optimization control strategy to achieve energy savings.

Based on the water pressure balance, the right pressure range and the opening position of balance valve can be determined by using the hydraulic model of a district heating system developed in this chapter.

This model will focus on the water pressure at every node within the pipeline network and pressure drop across every important device such as control valve, balance valve and terminal heater. First, it is necessary to calculate the water pressure distribution in the pipeline within this system in order to determine the relationship between pressure head and the length of pipe to the circulating pump. Second, it is important to calculate the pressure drop across the balance valves in order to find the relationship between the pressure drop across the balance valves and the outside temperature. Finally, a relationship between the balance valve opening and outside temperature will be determined.

In this chapter, the hydraulic calculations are performed in order to determine the necessary pressure heads of pumps within the pipeline network. The pump pressure heads should be high enough to provide sufficient hot water flow to the terminal heater in order to satisfy users' heating needs. But it should not be too high, because the surplus of the pressure head will be throttled by the flow control valves and such an operation leads to unnecessary energy losses. [24]

The steady state hydraulic method will be used to calculate hydraulic parameters in this model. In the district heating system thermal transients are slow with time constant of the order of hours. During these time periods, the water in the pipelines can be considered to be incompressible in regard to the pressure changes because the velocity of pressure wave propagations is very fast. The main pipelines' flow speed was set at 1.2m/s to 1.7m/s in this thesis. Based on the above assumption, the network hydraulics parameters such as pressure and flow rates distribution within the pipeline network were calculated by utilizing the classical rules of steady state hydraulics.

The pressure drop will be calculated due to friction and local losses. The diameter, length, absolute roughness of inside pipe wall, water density and kinematic viscosity data are assigned to each segment. The local friction factors of main pipes and branch pipes are also assigned to each segment and they are 0.2, 0.3 respectively. [7]

Considering the building height and other pressure constraints, the lowest water pressure will be chosen at makeup water point in order to keep supply and return water circulating normally. In this model, the water pressure at makeup water point will be assumed to be 253000Pa.

All pressure drops across the control valves will be related with corresponding mass flow water rate. Based on the pressure drop of balance valve 6 as the worst loop 6 (Figure 4.1), the pressure drops of other balance valves in other loops will be calculated. In addition, the balance valves opening positions will also be determined.

4.2 Hydraulic modeling

Based on the water mass flow rate and physical system parameters, such as diameter, length, roughness, etc. the water pressure distributions of whole hot water system at different outdoor temperature conditions are calculated. Moreover, the pressure drop across balance valves and the relationship with outdoor temperature are also presented in this chapter.

4.2.1 Water pressure model of DH system

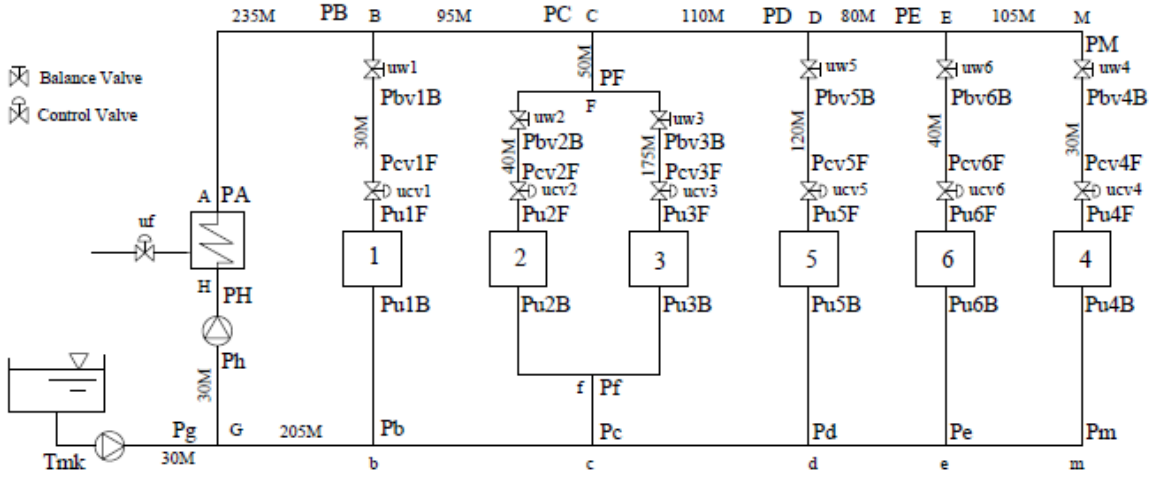

Figure 4.1 The schematic diagram of hydraulic system network

The water pressures at different points in this district heating system will be calculated with a 253KPa water pressure at the makeup water point.

In a closed loop system, the cyclic integral of pressure drops is equal to zero. Also the required pressure head of circulating pump equals the sum of the pressure drops in the worst loop.

For example: for the loop 6 (Figure 4.1), the required pressure head of circulating pump H_{req} is calculated as below:

$$H_{req} = \sum_{i=1}^{11} WR_i + PD_{bv6sp} + WR_{u6} + WR_{cv6} + WR_b \tag{4.1}$$

Where H_{req} = The required water pressure head of circulating pump, Pa

$\sum_{i=1}^{11} WR_i$ = The sum of water resistance of 11 pipe segments in loop 6, Pa

PD_{bv6sp} = The pressure drop set point of balance valve 6, it was set at 20KPa here.

WR_{u6} = The water resistance of terminal heater 6, Pa

WR_{cv6} = The water resistance of control valve 6, Pa

WR_b = The water resistance of boiler, Pa

Friction losses in the pipes are dependent on the fluid flow state such as laminar, transient and turbulent as determined by the Reynolds Number R_e [5]. To this end, the

different friction coefficient λ is selected to calculate the water resistance in each pipe segment and local friction of fittings in the pipe segment. The calculation procedure is presented in the example below:

For the pipe segment AB from point A to B (Figure 4.1), the velocity of water V_{wAB} is calculated by the equation shown as below:

$$V_{wAB} = 4m_{AB} / (\rho_w \pi D_{iAB}{}^2) \tag{4.2}$$

Where V_{wAB} = The velocity of water in pipe segment AB, m/s

m_{AB} = The water mass flow rate in pipe segment AB, Kg/s

ρ_w = The water density at average water temperature in pipe segment AB, kg/m^3

D_{iAB} = The inside diameter of pipe segment AB, m

The Reynolds Number R_e defined by the ratio of dynamic pressure ($\rho_w V^2{}_{wAB}$) and shearing stress ($\mu V_{wAB} / D_{hAB}$) for the pipe segment AB can be expressed as

$$R_e = \rho_w V_{wAB} D_{hAB} / \mu = V_{wAB} D_{hAB} / \upsilon \tag{4.3}$$

Where D_{hAB} = The hydraulic diameter of pipe segment AB, it equals inside diameter D_{iAB} of the pipe segment AB

μ = The dynamic viscosity at average temperature in Ns/m^2

υ = The kinematic viscosity at average temperature in m^2/s

The friction coefficient λ can be expressed as [7]

If $R_e \leq 2300$, $\lambda = 64 / R_e$ (4.4)

If $2300 < R_e < 10^5$, $\lambda = 0.3164 / R_e^{0.25}$ (4.5)

If $R_e \geq 10^5$, $\lambda = 0.11(K / D_h)^{0.25}$ (4.6)

Where D_h = The hydraulic diameter of pipe segment in m, it is equal to pipe inside diameter D_i.

K = The absolute roughness of inside pipe wall, it was assumed 0.0005m for all hot water distribution pipelines.

The ratio of water resistance of the pipe segment AB can be expressed as [7]

$$R_{pAB} = 6.25 \times 10^{-8} \lambda (3600 m_{AB})^2 / (\rho_w D_{iAB}^{\ 5}) \quad (4.7)$$

Where R_{pAB} = The ratio of water resistance of the pipe segment AB, in Pa/m

R_{eAB} = The Reynolds Number

The water resistance of pipe segment AB can be calculated as

$$WR_{AB} = L_{AB}(1 + \alpha) R_{pAB} \quad (4.8)$$

Where $\alpha = 0.2$, the minor friction rate of pipe segment AB. It was assumed to be 0.2 and 0.3 for the main pipe segments and the branch pipe respectively [7].

The resistance of the terminal heater 6 and the boiler were calculated as below [7]:

$$WR_{u6} = (u_{cv6} u_{bv6})^2 WR_{u6d} \tag{4.9}$$

$$WR_b = (m_{AB} / m_{ABd})^2 WR_{bd} \tag{4.10}$$

Where u_{cv6} = Normalized flow rate through the control valve 6

u_{bv6} = Normalized flow rate through the balance valve 6

WR_{u6d} = The water resistance of the terminal heater 6 under design condition, Pa

m_{AB} = The actual water mass flow rate in the pipe segment AB, kg/s

m_{ABd} = The design water mass flow rate in the pipe segment AB, kg/s

WR_{bd} = The water resistance of the boiler under design condition, Pa

The water resistance WR_{cv6} of the control valve 6 can be expressed as [27]

$$WR_{cv6} = 5 u_{cv6}^{-1} m_{E6}^{\ 2} / (2\rho_w (\pi / 4 D_{icv6}^{\ 2})^2) \tag{4.11}$$

Where m_{E6} = The actual frontal water mass flow rate into the control valve 6, in kg/s

D_{icv6} = The inside diameter of the control valve 6, in m

By using the above equations, the water pressure distribution in the pipeline was calculated and is shown below under different load conditions. Different load conditions were simulated at several outdoor temperatures. At each outdoor temperature, simulation runs were made to determine the boiler fuel input which maintains the zone air temperature at 18℃. Under these conditions, the corresponding mass flow rates and

pressure distribution in the system were determined. These results are presented in the following at four different (-15℃, -10℃, -5℃ and 0℃) outdoor air conditions:

1. In design condition, outside air temperature T_o =-15℃, the boiler water temperature is 78.17℃ (boiler fuel input $u_f = 0.813$); control valves are full open $u_{wi} = 1$ to achieve the zone air temperature set point of 18℃.

   Where $u_{wi} = u_{cvi} u_{bvi}$,

   u_{wi} = Normalized flow rate in the whole DH system

   u_{cvi} = Normalized flow rate in control valves

   u_{bvi} = Normalized flow rate in balance valves

The water pressure distribution obtained under the conditions is depicted in Figure 4.2.

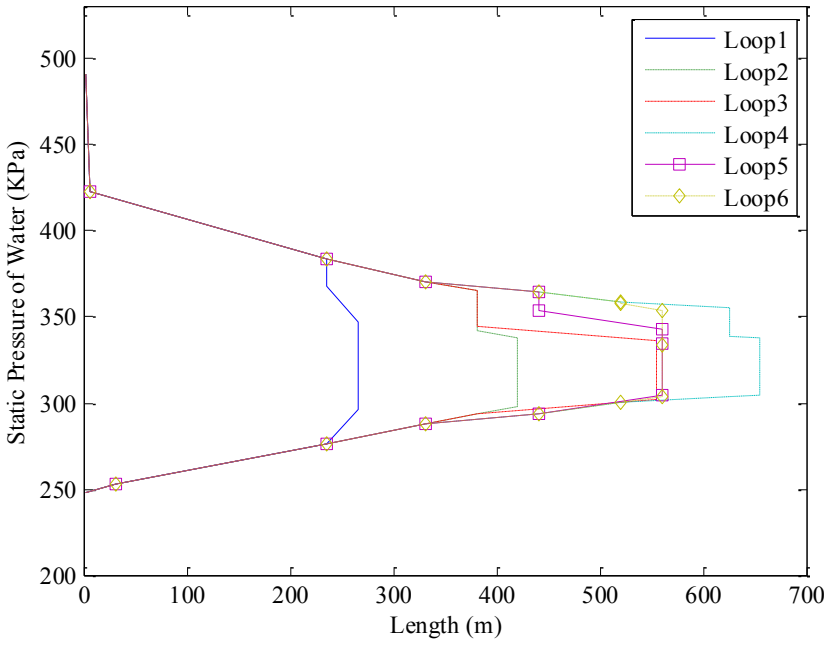

Figure 4.2 Water pressure distribution with $u_{wi} = 1$

2. The second simulation run was made under the following conditions: outside air temperature of T_o = -10℃, and the boiler water temperature held constant at 78.17℃ (the boiler fuel input $u_f = 0.712$); and control valves opening $u_{wi} = 0.602$ to achieve the zone air temperature set point of 18℃. The results are presented in Figure 4.3.

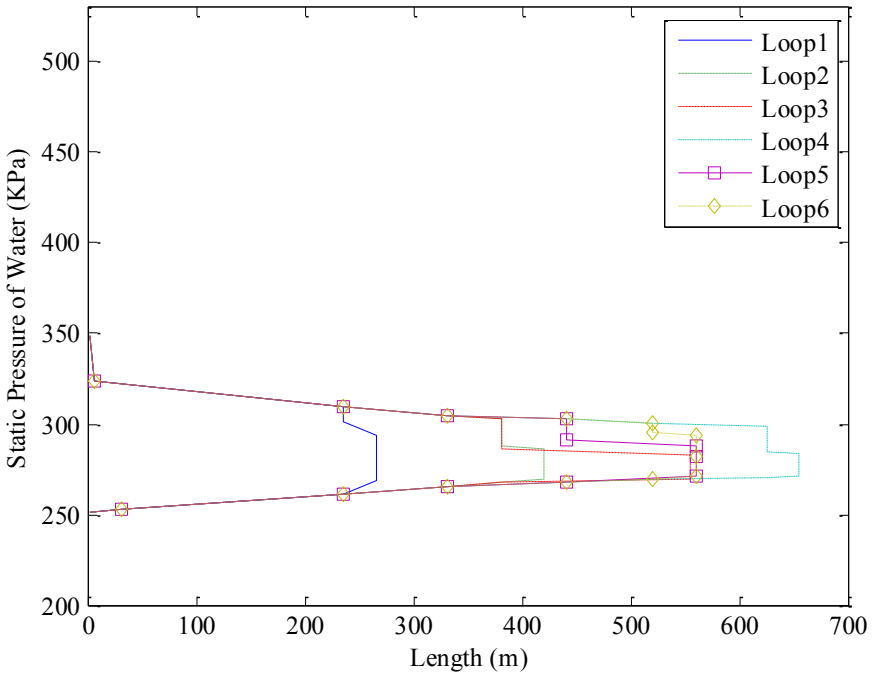

Figure 4.3 Water pressure distribution with $u_{wi} = 0.602$

3. The third simulation was made with an outside air temperature T_o = -5℃, the boiler water temperature is constant 78.17℃ (boiler fuel input $u_f = 0.624$); the control valves opening of $u_{wi} = 0.376$ was required to achieve the zone air temperature set point of 18℃. The resulting pressure distribution is shown in Figure 4.4.

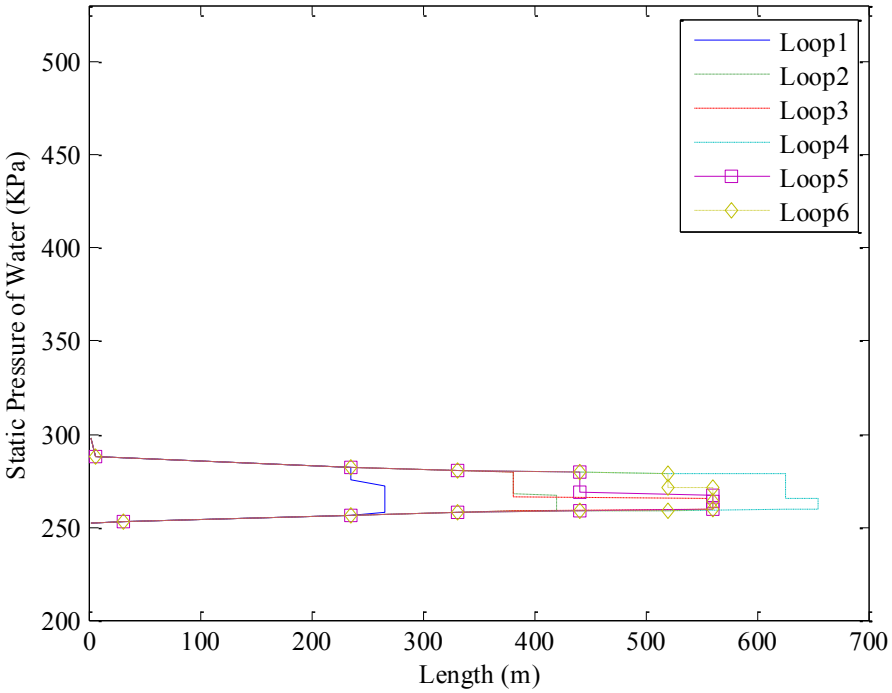

Figure 4.4 Water pressure distribution with $u_{wi} = 0.376$

4. Finally, the fourth simulation was made with an air temperature $T_o = 0$℃, the boiler water temperature is constant 78.17℃ (the boiler fuel input $u_f = 0.545$); the control valves opening of $u_{wi} = 0.238$ was required to achieve the zone air temperature set point of 18℃. The corresponding results are depicted in Figure 4.5.

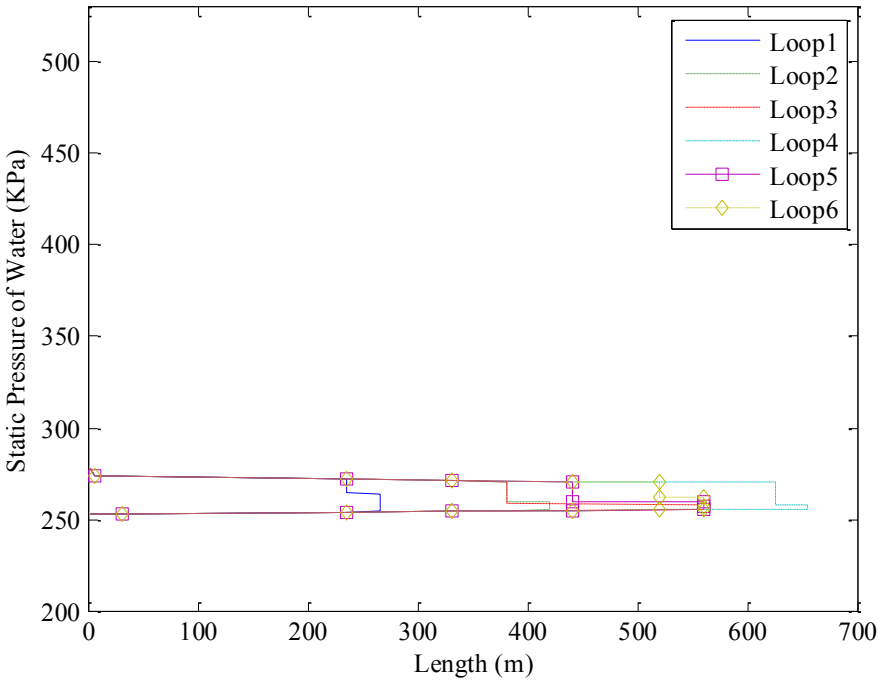

Figure 4.5 Water pressure distribution with $u_{wi} = 0.238$

From the figures shown above, it can be seen that water pressure drop is a function of pipeline length of the network. It can be noted that as the water mass flow rate is decreased by closing the valves the pressure drops also decrease. To this end, the required water pressure head of the circulating pump can be changed to match the desired water mass flow rate by using a suitable control strategy. It is also evident from the comparison of Figure 4.2-4.5, the circuit pressure drops or alternatively valve positions can be correlated with outdoor air temperature which directly impacts the building heating loads and consequently the water mass flow rate to satisfy a chosen indoor set point. Such a relationship is explored in the following set of results.

4.2.2 Balance valve water pressure drop

Based on the pressure drop of the balance valve in the worst loop, all other loop balance valve pressure drops can be calculated as follows:

$$PD_{bv1} = (WR_{BC} + WR_{CD} + WR_{DE} + WR_{E6} + PD_{bv6} + WR_{cv6} + WR_{u6} + WR_{6e} + WR_{ed} + WR_{dc} + WR_{cb}) - (WR_{B1} + WR_{cv1} + WR_{u1} + WR_{1b}) \quad (4.12)$$

$$PD_{bv2} = (WR_{CD} + WR_{DE} + WR_{E6} + PD_{bv6} + WR_{cv6} + WR_{u6} + WR_{6e} + WR_{ed} + WR_{dc}) - (WR_{CF} + WR_{F2} + WR_{cv2} + WR_{u2} + WR_{2f} + WR_{fc}) \quad (4.13)$$

$$PD_{bv3} = (WR_{CD} + WR_{DE} + WR_{E6} + PD_{bv6} + WR_{cv6} + WR_{u6} + WR_{6e} + WR_{ed} + WR_{dc}) - (WR_{CF} + WR_{F3} + WR_{cv3} + WR_{u3} + WR_{3f} + WR_{fc}) \quad (4.14)$$

$$PD_{bv4} = (WR_{E6} + PD_{bv6} + WR_{cv6} + WR_{u6} + WR_{6e}) - (WR_{E4} + WR_{cv4} + WR_{u4} + WR_{4e}) \quad (4.15)$$

$$PD_{bv5} = (WR_{DE} + WR_{E6} + PD_{bv6} + WR_{cv6} + WR_{u6} + WR_{6e} + WR_{ed}) - (WR_{D5} + WR_{cv5} + WR_{u5} + WR_{5d}) \quad (4.16)$$

The pressure drops of the control valves required in the above equations are calculated using the equations given below:

$$WR_{cv1} = 5u_{cv1}{}^{-1} m_{B1}{}^{2} / (2\rho_w (\pi / 4D_{icv1}{}^{2})^2) \quad (4.17)$$

$$WR_{cv2} = 5u_{cv2}{}^{-1} m_{F2}{}^{2} / (2\rho_w (\pi / 4D_{icv2}{}^{2})^2) \quad (4.18)$$

$$WR_{cv3} = 5u_{cv3}{}^{-1} m_{F3}{}^{2} / (2\rho_w (\pi / 4D_{icv3}{}^{2})^2) \quad (4.19)$$

$$WR_{cv4} = 5u_{cv4}{}^{-1} m_{E4}{}^{2} / (2\rho_w (\pi / 4D_{icv4}{}^{2})^2) \quad (4.20)$$

$$WR_{cv5} = 5u_{cv5}^{-1} m_{D5}^{2} / (2\rho_w (\pi / 4 D_{icv5}^{2})^2) \quad (4.21)$$

By using the above equations simulation runs were made to determine pressure drops across the balance and control valves as a function of normalized water mass flow rate u_{wi}. The results are shown in Figure 4.6. It can be seen that as the flow rate increases the pressure drop increases almost linearly as shown in the figure.

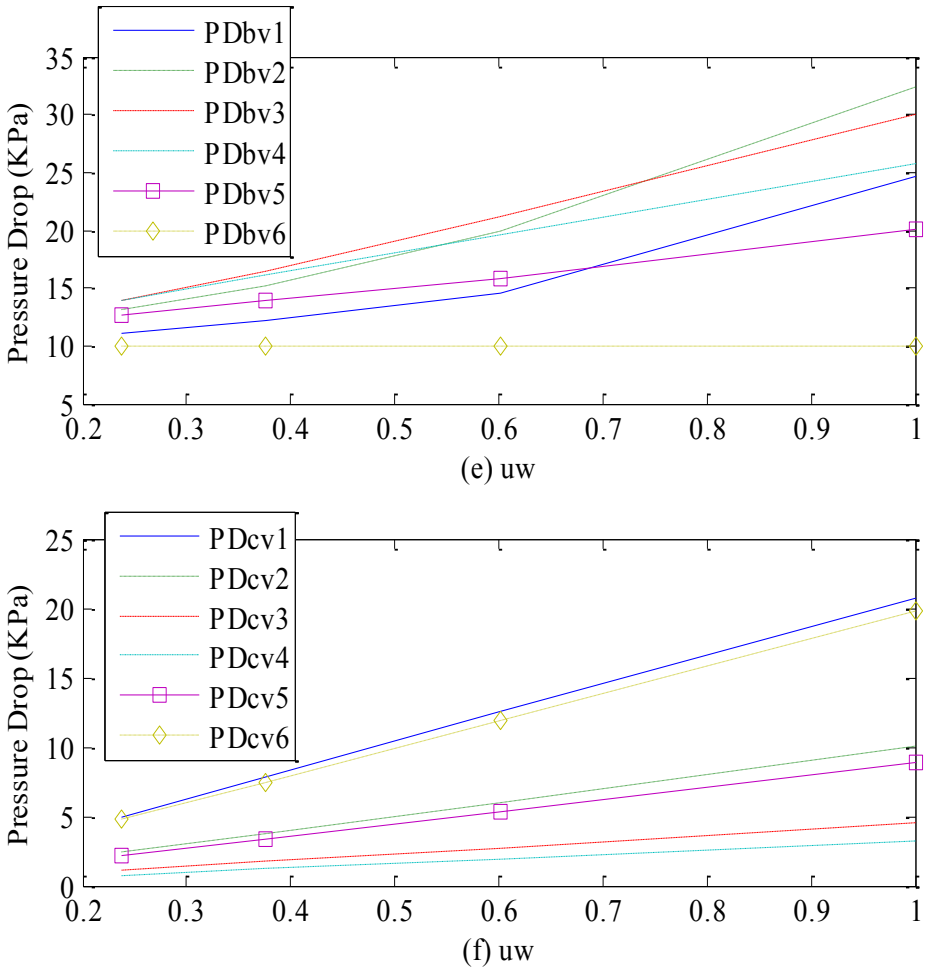

Figure 4.6 Valve pressure drop versus water mass flow rate

4.2.3 Balancing valves and evaluation procedure

The function of balance valve in a DH system is to balance the water resistance in each branch loop in order to achieve a reasonable distribution under design conditions. In this way, the balance valve can be used as a friction fitting which can be adjusted to satisfy the branch loop needs. In adjusting the balance valve position, the important factor to consider is pressure weighting factor of the branch loop which is defined as the ratio of balance valve pressure drop to the branch loop pressure drop. For good balancing, a weighting factor of 25-50% is recommended.

Also, the performance of balance valves is evaluated by factors such as cavitation.

Therefore the balance valve performance is dictated by the branch weighting factor subject to cavitation constraint. In the following, these two issues are discussed.

The branch pressure weighting factors as a function of heating load were determined by carrying out simulation runs at several outdoor air temperatures using equations 4.22-4.33. At each temperature the mass flow rate and consequently the pressure drop in each balance valve to maitain zone temperature of 18℃ was determined. The results are plotted in Figure 4.7(g). Also shown in Figure 4.7(h) is the branch pressure weighting factor as a function of outdoor air temperature. By using such curves it would be easier to select proper balance valve settings at a given temperature (or heating load).

The issue of cavitation erosion is usually difficult to model. However, manufactures of balance valve give empirical data to assess cavitaion constraint. Here, the method described in Reference [13] is briefly described.

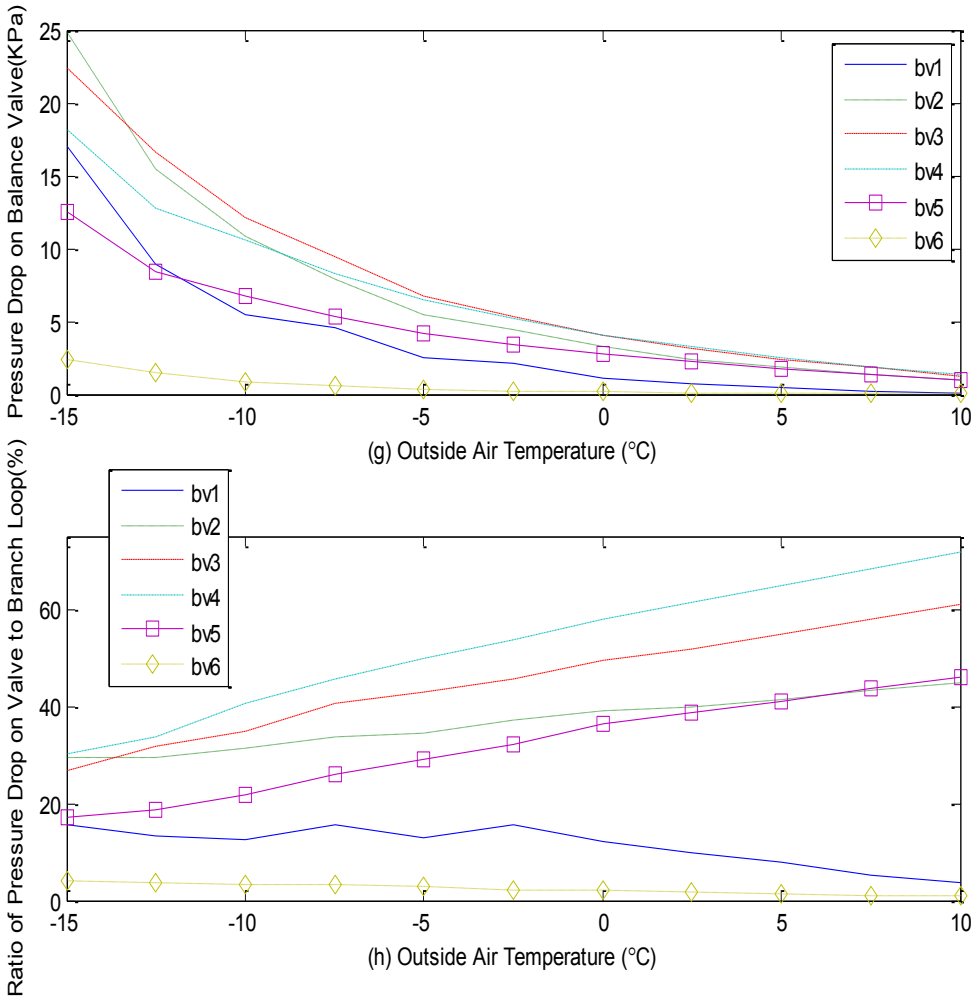

Figure 4.7 Balance valve pressure drop versus outdoor air temperature

Normally the ratio of pressure drop of the valve to branch loop is between 25%-50%.

$$PD_{bv1rat} = PD_{bv1} / (PD_{bv1} + WR_{B1} + WR_{cv1} + WR_{u1} + WR_{1b}) \tag{4.22}$$

$$PD_{bv2rat} = PD_{bv2} / (PD_{bv2} + WR_{CF} + WR_{F2} + WR_{cv2} + WR_{u2} + WR_{2f} + WR_{fc}) \tag{4.23}$$

$$PD_{bv3rat} = PD_{bv3} / (PD_{bv3} + WR_{CF} + WR_{F3} + WR_{cv3} + WR_{u3} + WR_{3f} + WR_{fc}) \quad (4.24)$$

$$PD_{bv4rat} = PD_{bv4} / (PD_{bv4} + WR_{E4} + WR_{cv4} + WR_{u4} + WR_{4e}) \quad (4.25)$$

$$PD_{bv5rat} = PD_{bv5} / (PD_{bv5} + WR_{D5} + WR_{cv5} + WR_{u5} + WR_{5d}) \quad (4.26)$$

$$PD_{bv6rat} = PD_{bv6} / (PD_{bv6} + WR_{B6} + WR_{cv6} + WR_{u6} + WR_{6e}) \quad (4.27)$$

For the butterfly balance valve, the limit values for preventing cavitation erosion are when $X_F > 0.25$ as well as when $\Delta P >$ 5 bar. Different type valves and their details are listed in table 4.1. [13]

The operating pressure ratio for all 6 balance valves are calculated as below:

$$X_{Fbv1} = PD_{bv1} / (P_B - P_v) \quad (4.28)$$

$$X_{Fbv2} = PD_{bv2} / (P_F - P_v) \quad (4.29)$$

$$X_{Fbv3} = PD_{bv3} / (P_F - P_v) \quad (4.30)$$

$$X_{Fbv4} = PD_{bv4} / (P_D - P_v) \quad (4.31)$$

$$X_{Fbv5} = PD_{bv5} / (P_E - P_v) \quad (4.32)$$

$$X_{Fbv6} = PD_{bv6} / (P_M - P_v) \quad (4.33)$$

Where X_F = Operating pressure ratio

P_v = Vapor pressure of water saturation at current temperature, in Pa

Valve design	$x_{Fcrit,cav}$ [-]	$\Delta p_{crit,cav}$ [bar]
Single-stage linear valves	0,7	15
Single-stage linear valves with stellited or hardened trim	0,7	25
3-stage linear valves	1,0	100
5-stage linear valves	1,0	200
Rotary plug valves	0,4	10
Butterfly and ball valves	0,25	5

Table 4.1 Limit values for preventing cavitation erosion [13]

In this method, there are two steps to verify whether or not cavitation will occur in a balance valve.

First, calculate the required valve angle using the flow coefficient data C_v ($C_v = Q/\sqrt{\Delta P}$) for the balance valve. By finding the percent of full open C_v from Figure 4.8, the valve position in degrees can be read from the figure.

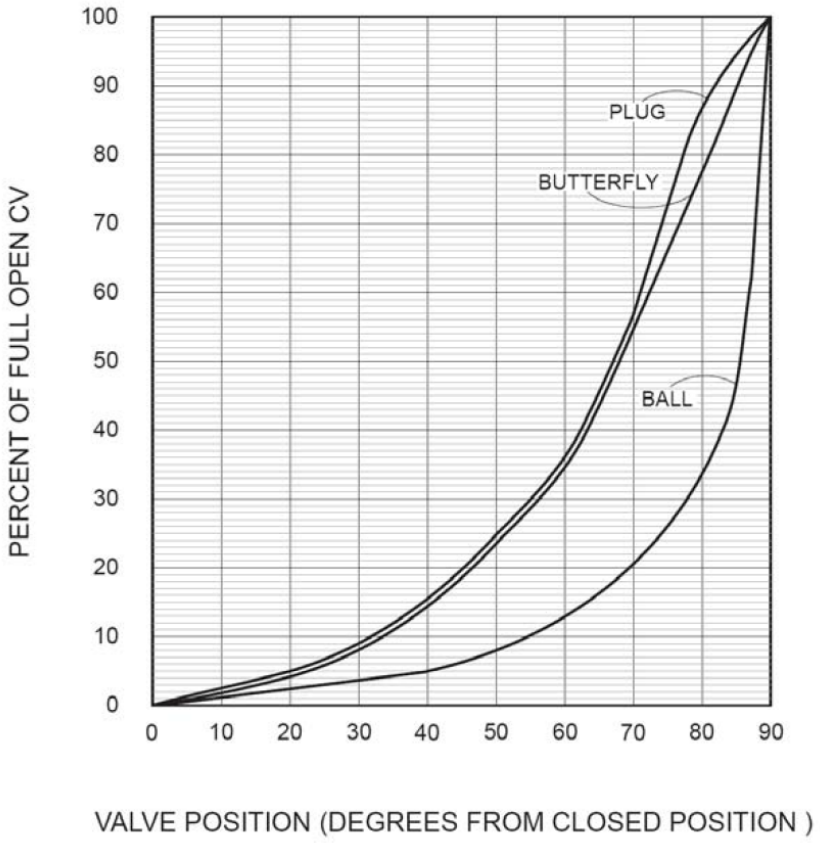

Figure 4.8 Flow Characteristics of Valves [23]

Second, the cavitation coefficient σ ($\sigma = 1/X_F$) is obtained from the figure 4.9. Figure 4.9 shows the safe operating and the cavitation zones. If the cavitation coefficient falls below the applicable valve curve, then cavitation will occur and the valve position is unsuitable. It means this position should be avoided in the actual operation in order to protect the valves in the system.

Therefore, it is important to check for this constraint in setting the balance valve positions in the branch loops.

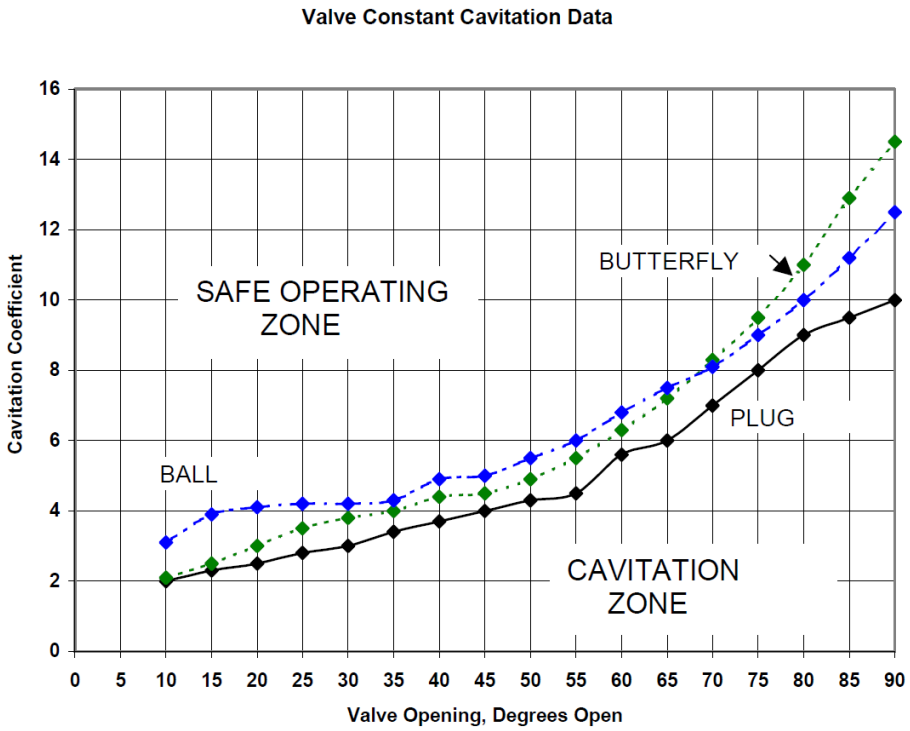

Figure 4.9 Cavitation Characteristics of Valves [23]

4.3 Balancing valve opening position as a function of outside temperature

The linear characteristic of balance valve opening and pressure drop is assumed in this model. Combining this with the flow characteristics of the balance valve, the balance valves opening can be expressed by empirical formula as below:

$$u_{bvr1} = (4m_{B1}{}^2 / (2\rho_w(\pi / 4D_{ibv1}{}^2)^2)) / PD_{bv1} \tag{4.34}$$

$$u_{bvr2} = (4m_{F2}{}^2 / (2\rho_w(\pi / 4D_{ibv2}{}^2)^2)) / PD_{bv2} \tag{4.35}$$

$$u_{bvr3} = (4m_{F3}{}^2 / (2\rho_w(\pi / 4D_{ibv3}{}^2)^2)) / PD_{bv3} \tag{4.36}$$

$$u_{bvr4} = (4m_{E4}{}^2 / (2\rho_w(\pi / 4D_{ibv4}{}^2)^2)) / PD_{bv4} \tag{4.37}$$

$$u_{bvr5} = (4m_{D5}{}^2 / (2\rho_w(\pi / 4D_{ibv5}{}^2)^2)) / PD_{bv5} \quad (4.38)$$

$$u_{bvr6} = (4m_{E6}{}^2 / (2\rho_w(\pi / 4D_{ibv6}{}^2)^2)) / PD_{bv6} \quad (4.39)$$

By using the above equations simulation runs were made at different outdoor air temperatures and corresponding mass flow rates. The results are depicted as a function of relative open position in Figure 4.10. These results can be used to reposition the balance valves at different outdoor temperatures.

The relative position of the balance valve in Figure 4.10 was defined as the ratio of actual pressure drop in the balance valve to pressure drop in the balance valve adjusted based on the worst loop pressure drop. The results presented in figure show that there is significant room for re-adjusting the balance valves periodically based on building heating loads which are mainly dependent on outdoor air temperatures.

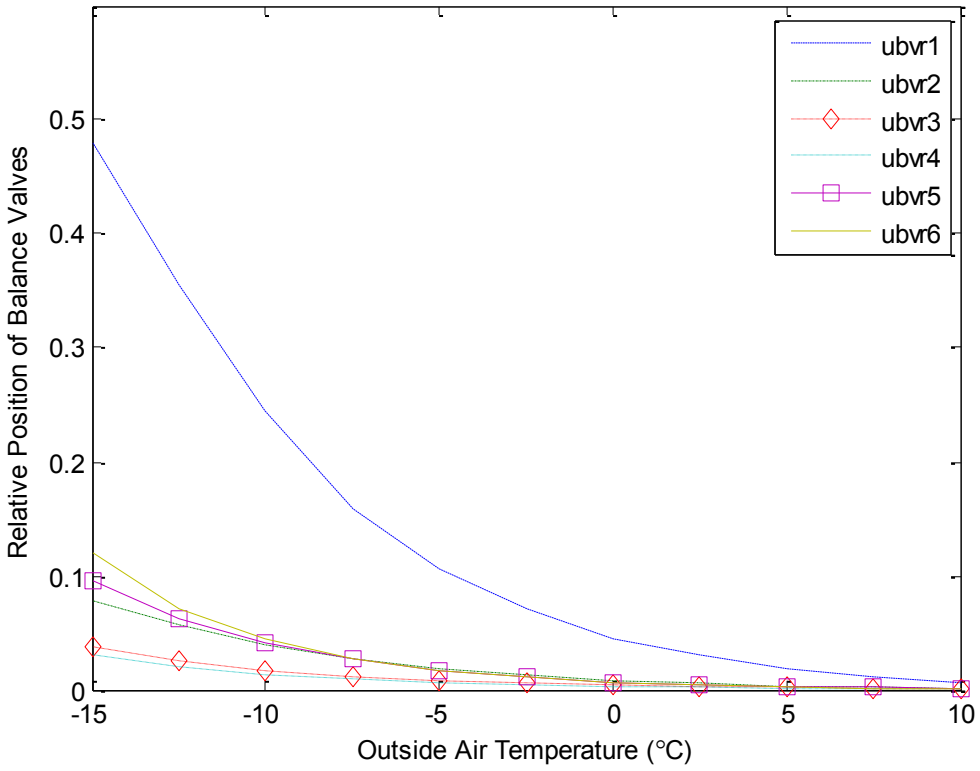

Figure 4.10 Balance valve opening with outdoor air temperature

4.4 Summary

A static hydraulic model of DH system has been developed in this chapter. It includes the water pressure distribution in DH system, water pressure drop of control and balance valves, balance valve working performance evaluation and balance valve opening position as a function of outdoor air temperature.

All hydraulic network calculations in this chapter are presented in steady state since the velocity of pressure wave propagation is very fast compared with the thermal transient responses.

Through this model, the water pressure of all important points in the pipe network can established. Also the model is capable of simulating pressure drops across balance valves and the pipe network under different hydraulic conditions.

The important result in this chapter is the relationship between balance valve relative position and outdoor air temperature. Based on this result, the different balance valve opening set points will be chosen under different weather conditions in order to study energy efficiency of system as described in the next chapter.

CHAPTER 5

A PI control strategy and energy optimal operation of DH system with balancing valve set points

5.1 Introduction

In order to improve energy efficiency of district heating systems it is important to develop optimal control and operation strategies under realistic operating conditions.

In this chapter, a PI (proportional-integral) control strategy will be designed for zone air temperature and boiler water temperature control. The PI control strategy is expected to keep the temperatures constant at their respective set points. As a result, the supply water mass flow rate variations as a function of outdoor temperatures will be monitored.

There are two factors which directly affect the thermal energy delivered from the boiler to the zone: these are water mass flow rate and water temperature respectively. Hence the optimization of these two variables will be studied to determine how to minimize the system energy consumption and to optimize the supply water set point temperature and mass flow rate under real outdoor air temperature conditions.

In the overall energy optimization of DH system, it is important to consider both boiler energy consumption and pump energy consumption. In this study both boiler energy and pump energy consumption as a function of heating loads are studied and optimized.

To this end, first the boiler energy consumption at different supply water temperature set points with outdoor air temperature is studied.

Furthermore, the effect of different balance valve opening positions as a function of outdoor air temperature on electric power consumption of circulating pump is studied.

It is noted that most current balance valves used in actual field are adjusted manually and always remain fixed at their initial balance position over the entire season. In this study the impact of changing the balancing valve position as a function of heating load are examined. In the following five different case studies are presented which cover from coldest to warm weather conditions and their impact on energy consumption are summarized.

5.2 PI control of boiler

In this closed control loop, shown in Figure 5.1, the error between the actual water temperature and set point temperature is used to adjust the fuel firing rate of the boiler. By feeding back the actual temperature monitored by the temperature sensor, the controller-actuator acts continuously to keep the boiler water temperature more and more near the set point.

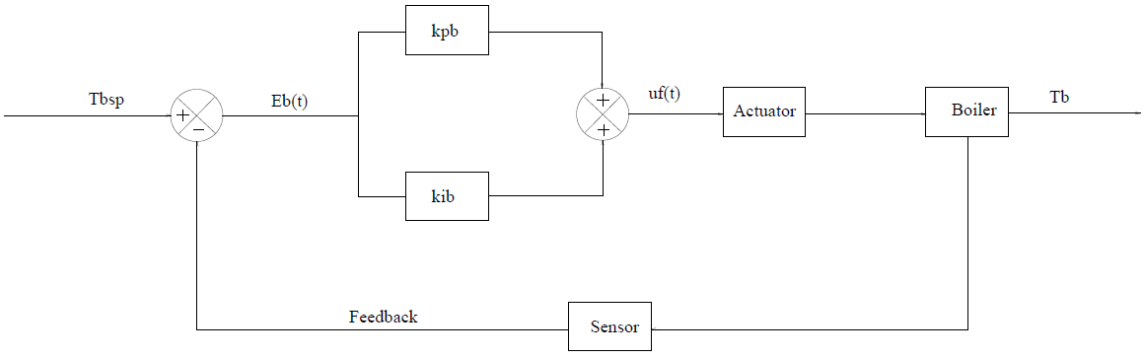

Figure 5.1 PI controller block diagram of boiler

The PI control equations are given below:

$$E_b(t) = T_{bsp} - T_b \tag{5.1}$$

$$u_f(t) = k_{pb}E_b(t) + k_{ib}\int_0^t E_b(t)dt \tag{5.2}$$

Where k_p = The proportional gain, and its magnitude was set at 1.0

k_i = The integral gain, 0.00001

T_{bsp} = The boiler water temperature set point, in ℃

u_f = The control variable of fuel input expressed as a percentage of full open position.

5.3 PI control of zone

The zone air temperature was controlled by a PI controller to modulate the water flow rate in the terminal heater. By feeding back the actual zone temperature to the controller, the control valve acts continuously to keep the zone air temperature near the set point. The closed loop PI control diagram for one single zone is depicted in Figure 5.2. The same control structure was employed for the remaining five zones.

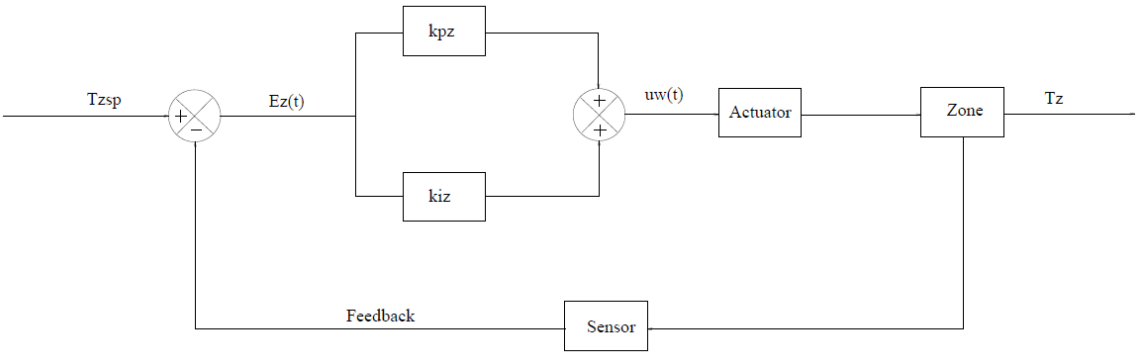

Figure 5.2 PI controller block diagram of zone

The corresponding PI control equations with controller gain values are shown below.

$$E_z(t) = T_{zsp} - T_z \tag{5.3}$$

$$u_w(t) = k_{pz}E_z(t) + k_{iz}\int_0^t E_z(t)dt \tag{5.4}$$

Where $k_p =$ the proportional gain was set at 0.8

$k_i =$ The integral gain value was 0.00001

$T_{zsp} =$ The zone air temperature set point, in ℃

$u_w =$ The control variable of control valve normalized with respect to full open position.

5.4 PI control of DH system

There are 6 buildings in this system. For simplicity, these buildings can be treated as six zones. So there are 6 PI controllers installed in 6 loops to control building air temperatures. By adjusting the water mass flow rate with control valve in each loop, each building zone air temperature can be kept at the desired set point.

Also there is one PI controller for the boiler. By adjusting the fuel input to the boiler, the supply water temperature can be kept at its set point value.

The PI control loops in DH system are shown in figure 5.3.

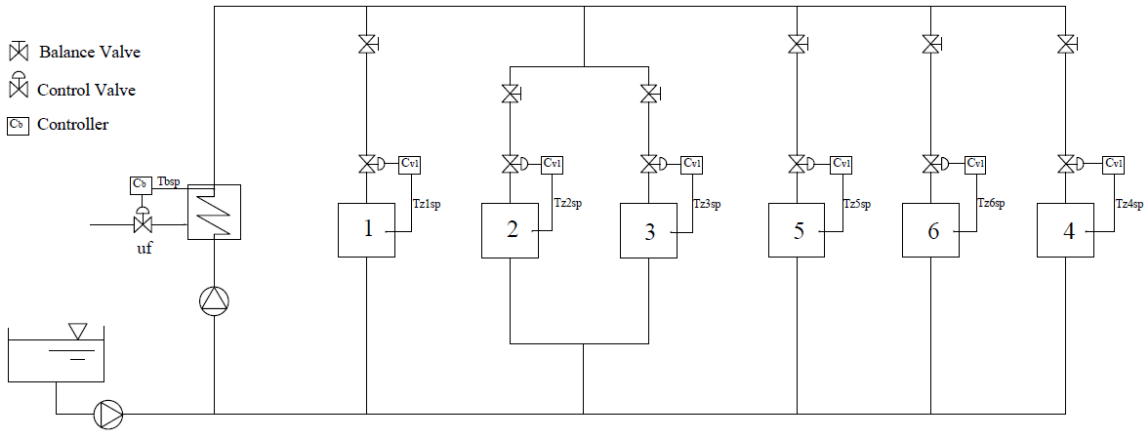

Figure 5.3 PI controller block diagram of DH system

5.5 PI control responses of DH system

A typical day outdoor air temperature profile was used to simulate and study the PI control responses of DH system. In this simulation the boiler water temperature was controlled by modulating fuel firing rate in the boiler. The zone temperatures were allowed to float. In other words, zone temperatures were not controlled. This simulation

is intended to show what the impact of controlling boiler water temperature is on the open loop control of zone temperatures. Figure 5.4 shows the temperature responses.

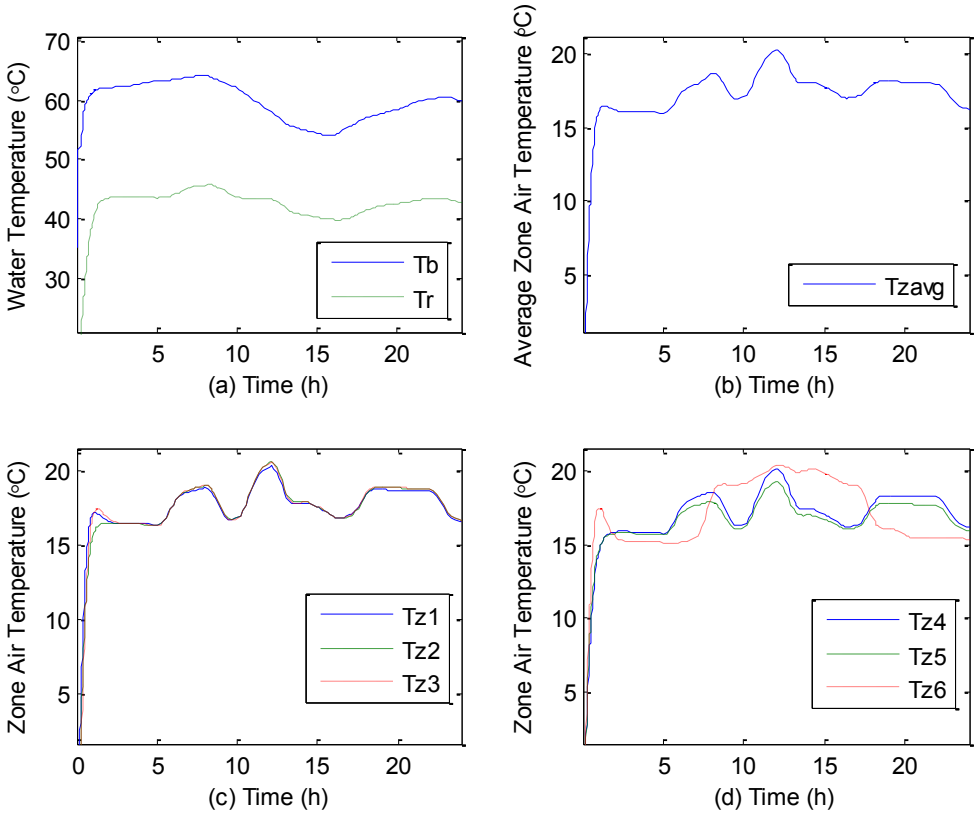

Figure 5.4 Temperature response in normal condition with heat gain and loss and u_f is controlled

From figure 5.4, it can be seen that the boiler water temperature supplied to this system response is much better than in the previous open loop response shown in Figure 3.8. This is due to the fact that boiler supply water temperature is set as a function of outside air temperature and the fuel input is controlled as a function of outdoor air temperature. As a consequence, the zone air temperatures variations are also minimized compared to those shown in Figure 3.8.

Although the zone temperature variations are not excessive under open loop control, but from a practical point of view zone temperatures have to be controlled to maintain occupant thermal comfort conditions under variable loads. To this end, water mass flow rate to each terminal heater in the zone were controlled using PI controllers. Thus in the simulations both boiler and six zones output temperatures were controlled. A typical day responses are depicted in Figure 5.5.

From figure 5.5(a), it is clear that the boiler water temperature is kept close to its set point 76℃ after 7 hours and the return water temperature is varying along with the mass flow rate as the control valves modulate in response to changes in outdoor air temperature.

From figure 5.5(b), it is clear that the zone air temperatures are much closer to set point 18℃ even though the outdoor air temperature is changing continuously.

Figure 5.5(c), (d) show that the control signal for boiler fuel input and water flow rate responses with outdoor air temperature over the 24 hour period. The boiler fuel firing rate varies between 0.6 to 0.75 most of the day and water mass flow rate varies from 0.4 to 0.6 of the maximum mass flow rate.

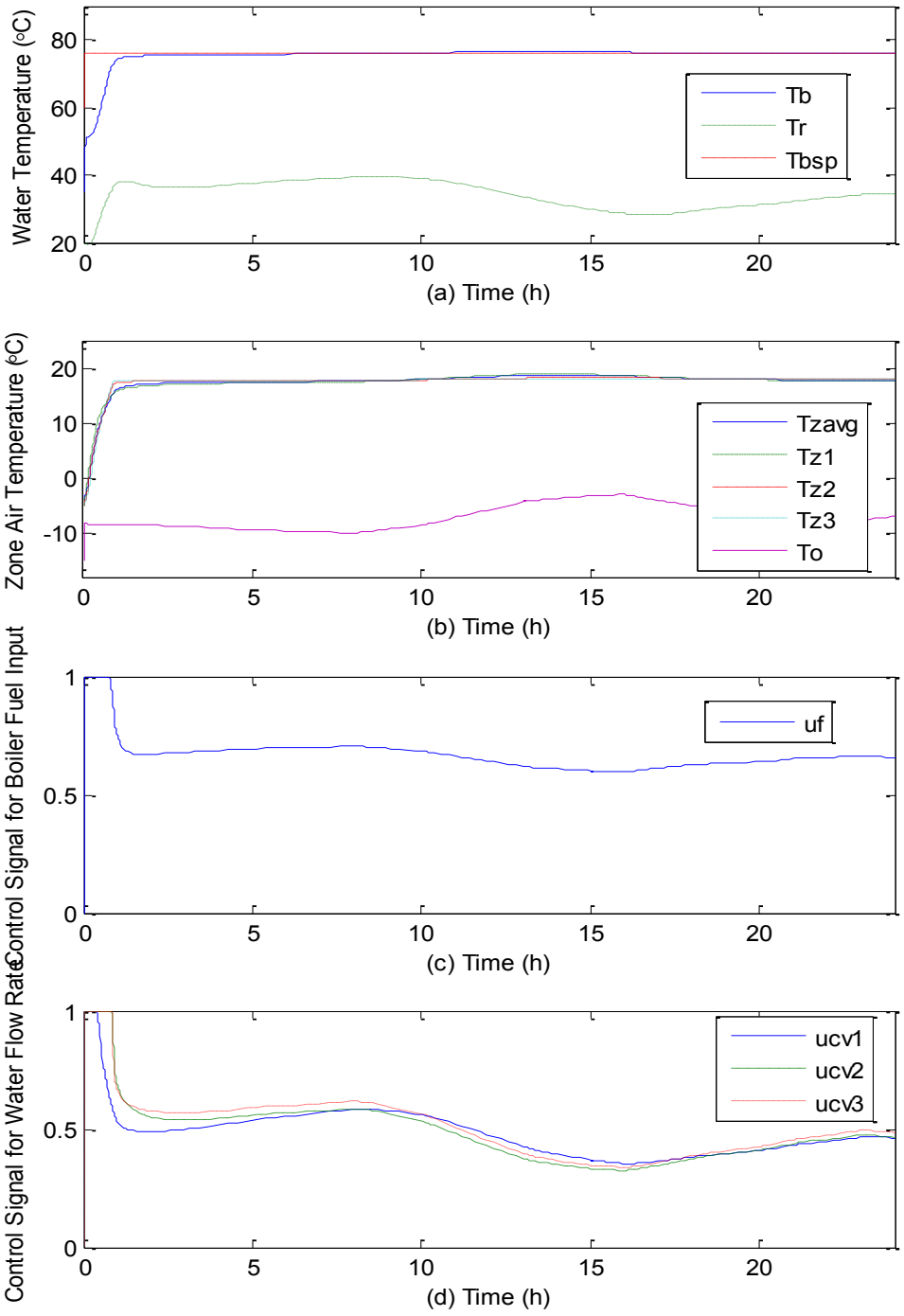

Figure 5.5 PI control responses of DH system

5.6 Optimization of PI control set points

Choosing optimal set points for the boiler water temperature is very important for improving the energy efficiency of DH systems. The optimized set points will achieve significant energy saving in practice. Hence, a multi-variable constrained optimization approach is developed to obtain optimal operating set points based on different weather conditions as described below [Li][26]. To simplify the optimization problem, the overall DH system was considered as an aggregated single zone heated by the boiler. The energy balance on the assumed aggregated model is described in Equations 5.7-5.8. The major objective of this model is to seek optimal supply water temperatures that minimize boiler energy consumption.

To this end, first, five variables such as T_s , T_r , T_z , u_w , u_f are established in this model and their upper and lower bounds are chosen as given below:

Lower bounds= [30, 20, 18, 0.2, 0]

Upper bounds= [95, 70, 19, 1, 1]

Second, the equality constraints are expressed with the following equations:

$$u_f m_{f\max} e_b HV = c_w u_w m_{bd} (T_s - T_r) \tag{5.5}$$

$$U_{htr}(0.5(T_s + T_r) - T_z)^{(1+c_{htr})} = c_w u_w m_{bd} (T_s - T_r) \tag{5.6}$$

$$U_{en}(T_z - T_o) = c_w u_w m_{bd} (T_s - T_r) \tag{5.7}$$

Where $u_w = u_{cv} u_{bv}$

Third, the objective function is described as cost function using equation (5.8) through which energy consumption will be minimized.

$$J_{\min} = \int_0^t [c_w u_w m_{bd} (T_s - T_r)] dt \tag{5.8}$$

By using the MATLAB tool box, the optimal set points of water temperature were found at different outdoor air temperature conditions as shown in Figure 5.6.

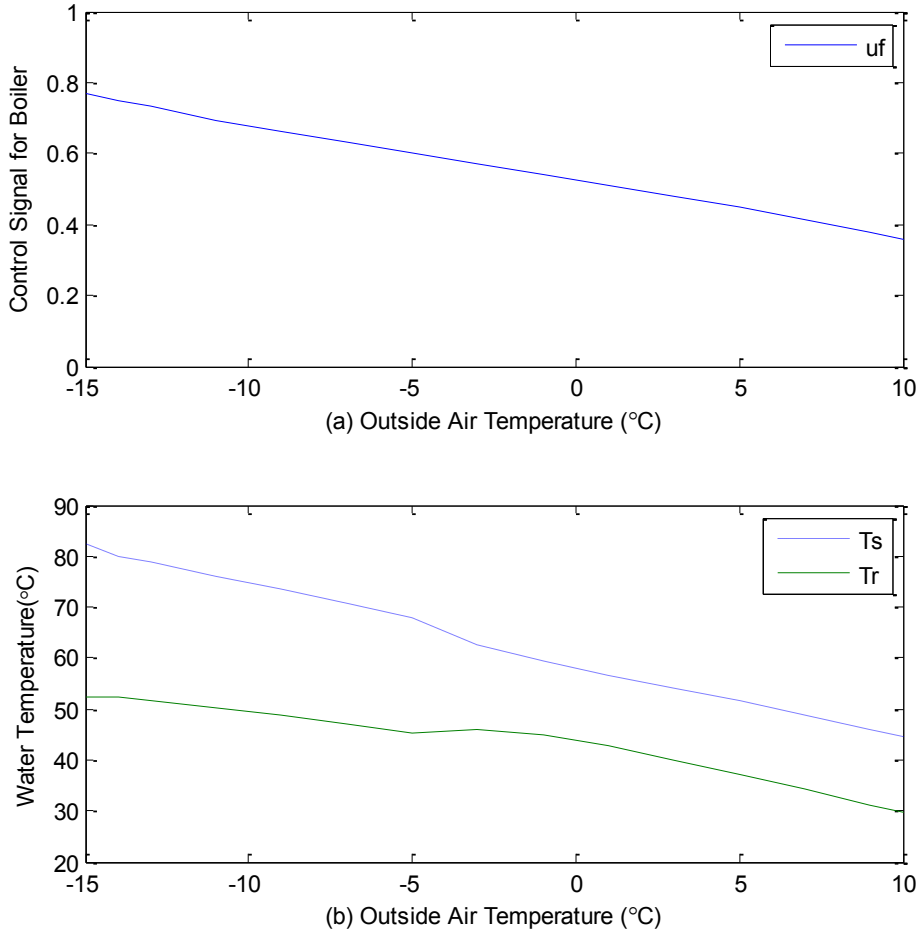

Figure 5.6 Optimization of PI control set points

Figure 5.6 shows that the optimal set points of supply water temperature as a function of outdoor air temperature to keep the zone air temperature constant at 18℃. It can be noted that both supply and return water temperatures gradually decrease as the outdoor temperature increases. At 10℃ the supply temperature is close to 45℃ which is close to one half of the full load supply temperature value of about 82℃.

5.7 Near-Optimal balance valve settings

By using the optimal supply water temperatures at different outdoor air temperatures (Figure 5.6), the corresponding balance valve positions satisfying the optimal supply water set point, zone temperature set points were obtained. These near-optimal settings are depicted in Figure 5.7 and these were used to compute energy consumption for optimal control strategy. As can be seen from the figure, balance valves need resetting at partial load conditions under mild outdoor temperatures.

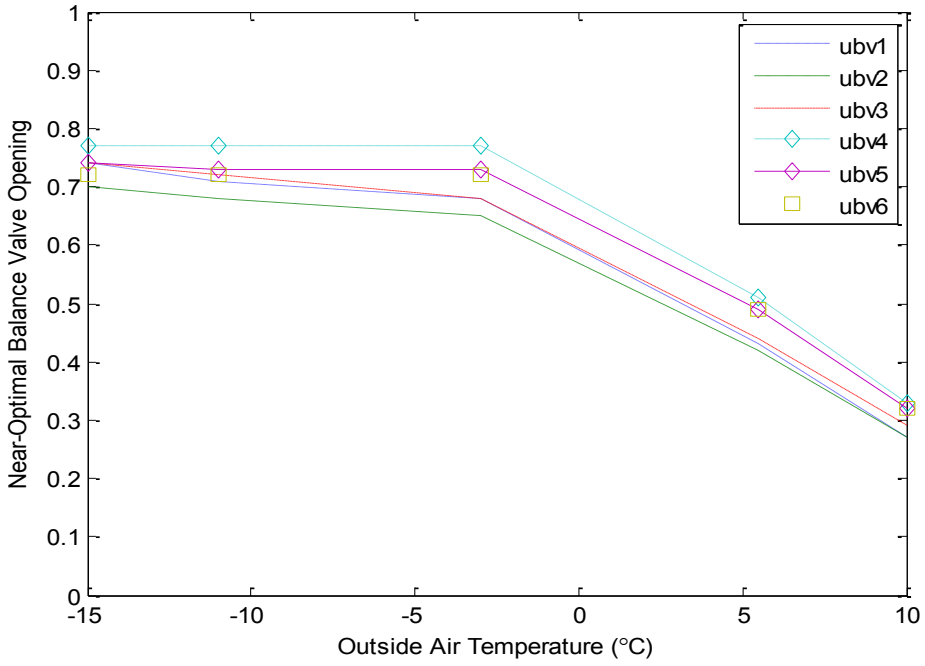

Figure 5.7 Near-Optimal balance valve position as a function of outdoor air temperature

5.8 Comparison of energy consumption under different weather conditions

Simulation runs were made using the overall DH system model to study energy consumption under different load and control strategies. To this end the method used to calculate the energy consumption is described.

The energy consumption of DH system consists of fuel consumption of boiler E_b (GJ) and electrical power consumption of circulating pump E_p (KWh). These two types of energy calculations are expressed by the equations given below:

$$E_b = 10^{-9} * \int_0^t (Q_{bd} u_f e_b / e_{\max}) dt \tag{5.9}$$

$$E_p = \int_0^t [9.81 d_w (3.6 m_{gh})(10^{-4} P_{Hpump}) / (3.6 * 10^6 e_{pump} e_{motor})] dt \tag{5.10}$$

Where P_{Hpump} = The pressure head of circulating pump, in Pa

e_{pump} = The efficiency of circulating pump,

e_{motor} = The efficiency of electric motor

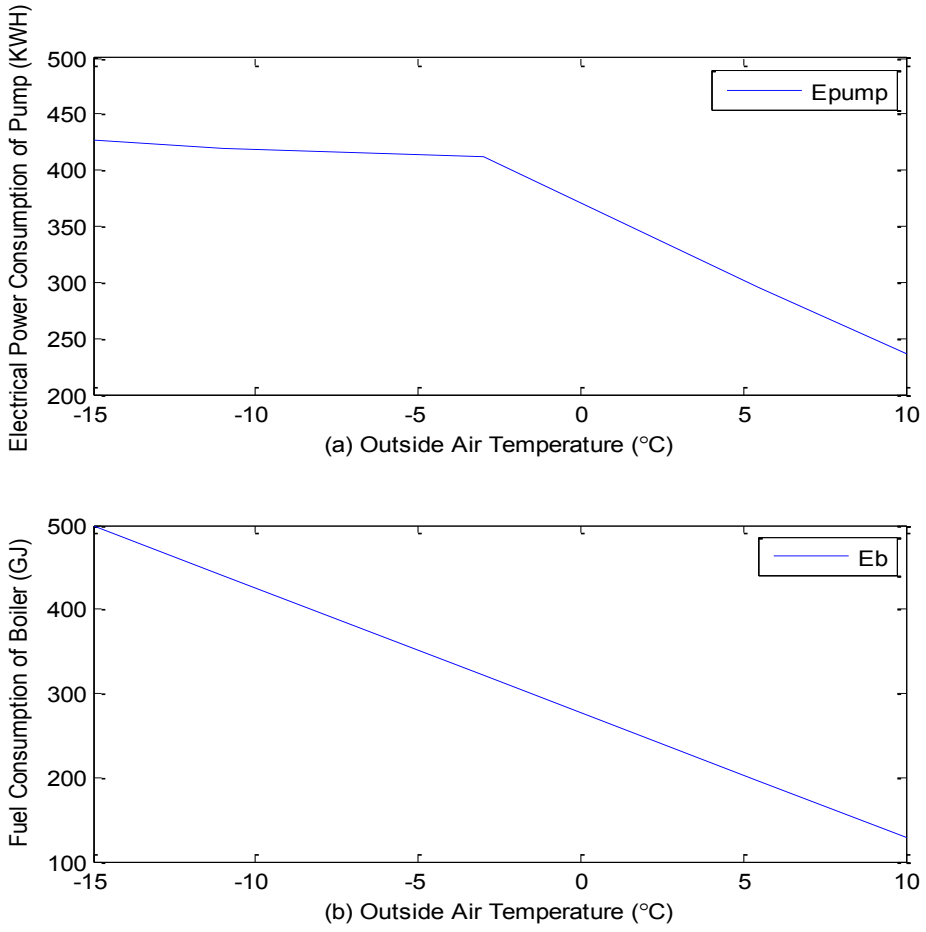

Figure 5.8 Daily energy consumption with optimal set points

Figure 5.8 shows that the energy consumption including fuel and electrical power during 24 hours period as a function of outdoor air temperature. As shown in Figure 5.8 it is clear that pump energy savings will be more pronounced in warm weather than in the cold weather conditions. These results correspond to optimal control strategy.

In the following energy consumption of DH system under different weather conditions is studied. The simulation results are summarized in Table 5.1. The five cases include a base case and four cases corresponding to cold to warm weather conditions including solar radiation and internal heat gains.

Each simulation was done over a 24-hour period. The outdoor air temperature was assumed in three ranges from coldest to warm to simulate seasonal changes. The coldest range was from -15℃ to -7℃, cold range was from -7℃ to 2℃ and warm temperature range was from 2℃ to 10℃. Three outdoor air temperature profiles covering the above ranges were used in the simulation runs.

Also, the disturbances including the variation in solar radiation and internal heat gain corresponding to residential and commercial building schedule were considered in this comparison.

The results of comparison are shown in table 5.1.

Coldest Period (T_o =-7～-15℃),To=RealOutsideTemp1(t),solar radiation,internal gain,24Hours										
Case No.	T_{bsp}	u_{bvi}	u_{cvi}	T_{zi}		T_s	T_r	u_f	E_p (Kwh)	E_b (GJ)
Base Case	$T_{bsp}=f(T_o)$	1	1	T_{zi}	17.91~ 18.94	65.85	47.29	0.62	580.42	431.93
				T_{zavg}	18.54					
Case 1	$T_{bsp}=f(T_o)$	u_{bvi} = fixed(coldest position)	1	T_{zi}	17.49~ 18.54	65.82	45.88	0.61	535.32	425.88
				T_{zavg}	18.21					
Case 2	$T_{bsp}=f(T_o)$	$u_{bvi}=f(T_o)$	1	T_{zi}	17.49~ 18.54	65.82	45.88	0.61	535.32	425.88
				T_{zavg}	18.21					
Case 3	$T_{bsp}=f(T_o)$	$u_{bvi}=f(T_o)$	PI	T_{zi}	17.58~ 17.76	65.80	42.17	0.61	399.81	400.00
				T_{zavg}	17.70					
Case 4	$T_{bsp}=T_{bopt}$	$u_{bvi}=u_{bviopt}$	PI	T_{zi}	17.92~ 18.02	75.99	38.03	0.64	340.58	399.34
				T_{zavg}	17.97					

Cold Period (T_o =-7～2℃),To=RealOutsideTemp2(t),solar radiation, internal gain,24Hours										
Case No.	T_{bsp}	u_{bvi}	u_{cvi}	T_{zi}		T_s	T_r	u_f	E_p (Kwh)	E_b (GJ)
Base Case	$T_{bsp}=f(T_o)$	1	1	T_{zi}	17.26~ 18.61	51.00	40.91	0.44	580.42	322.91
				T_{zavg}	18.21					
Case 1	$T_{bsp}=f(T_o)$	u_{bvi} = fixed(coldest position)	1	T_{zi}	17.29~ 18.53	50.99	40.04	0.44	535.32	318.47
				T_{zavg}	18.06					
Case 2	$T_{bsp}=f(T_o)$	$u_{bvi}=f(T_o)$	1	T_{zi}	17.33~ 18.38	50.97	39.03	0.44	489.88	313.54
				T_{zavg}	17.93					

Case 3	$T_{bsp} = f(T_o)$	$u_{bvi} = f(T_o)$	PI	T_{zi}	17.47~ 17.77	50.95	36.12	0.44	362.72	291.56
				T_{zavg}	17.66					
Case 4	$T_{bsp} = T_{bopt}$	$u_{bvi} = u_{bviopt}$	PI	T_{zi}	18.00~ 18.12	62.56	34.57	0.49	331.65	291.04
				T_{zavg}	18.06					

Warm Period (T_o =2～10℃),To=RealOutsideTemp3(t),solar radiation, internal gain,24Hours										
Case No.	T_{bsp}	u_{bvi}	u_{cvi}	T_{zi}		T_s	T_r	u_f	E_p (Kwh)	E_b (GJ)
Base Case	$T_{bsp} = f(T_o)$	1	1	T_{zi}	17.16~ 18.60	37.02	32.63	0.28	580.42	188.50
				T_{zavg}	18.19					
Case 1	$T_{bsp} = f(T_o)$	u_{bvi} = fixed(coldest position)	1	T_{zi}	17.18~ 18.52	37.02	32.22	0.28	535.32	186.03
				T_{zavg}	18.14					
Case 2	$T_{bsp} = f(T_o)$	$u_{bvi} = f(T_o)$	1	T_{zi}	17.26~ 18.43	37.01	30.85	0.29	428.58	178.81
				T_{zavg}	18.04					
Case 3	$T_{bsp} = f(T_o)$	$u_{bvi} = f(T_o)$	PI	T_{zi}	17.40~ 17.88	37.00	27.85	0.29	297.39	158.27
				T_{zavg}	17.73					
Case 4	$T_{bsp} = T_{bopt}$	$u_{bvi} = u_{bviopt}$	PI	T_{zi}	18.03~ 18.16	50.88	22.85	0.36	238.77	157.72
				T_{zavg}	18.10					

Table 5.1 Daily energy consumption comparison

In Table 5.1 the daily energy consumption obtained under four different operating strategies, referred to as case 1 through case 4, are compared with the base case energy

consumption (the base case). The different operating strategies simulated were defined as follows:

1. Base case:

   Boiler: Outdoor air reset control

   Zones: Open-loop (no control)

   Balance valves: Full open

   Outdoor air temperature: Design day condition

2. Case 1:

   Boiler: Outdoor air reset control

   Zones: Open-loop (no control)

   Balance valves: Valve settings based on design day conditions

   Outdoor air temperature: Variable

3. Case 2:

   Boiler: Outdoor air reset control

   Zones: No control

   Balance valves: Valve settings based on outdoor temperature (Figure 4.10)

   Outdoor air temperature: Variable

4. Case 3:

   Boiler: Outdoor air reset control

   Zones: PI control

   Balance valves: Valve settings based on outdoor temperature (Figure 4.10)

   Outdoor air temperature: Variable

5. Case 4:

   Boiler: PI control to maintain optimal set points

   Zones: PI control

   Balance valves: Valve settings based on optimization (Figure 5.7)

   Outdoor air temperature: Variable

In each of the above case, disturbances due to solar and internal heat gain were considered.

From table 5.1, it is easier to see that electrical power consumption of circulating pump is governed by the water mass flow rate variations occurring in different cases. That means the balance valve opening position directly influences the energy consumption of the pump. The highest percent of electrical power saving is 55.4% which is due to optimal position of the balancing valve compared with the base case opening position. At the rate $0.1/KWh, the maximum and minimum energy consumed by the circulating pump translates into $58/day to $24/day which is less than half of energy cost compared to the base case.

Also, the fuel consumption is mainly dependent on supply water temperature set point. It shows that the total fuel consumption in 24 hours under warm period is decreased by more than 61% compared to the coldest period. A graphical result of these energy consumptions are depicted in Figure 5.9(a-c).

The results presented above are particularly significant in that they highlight the impact of balance valve settings on pump energy consumption. Implementations of results

presented here in real buildings are expected to yield significant savings in pump energy costs.

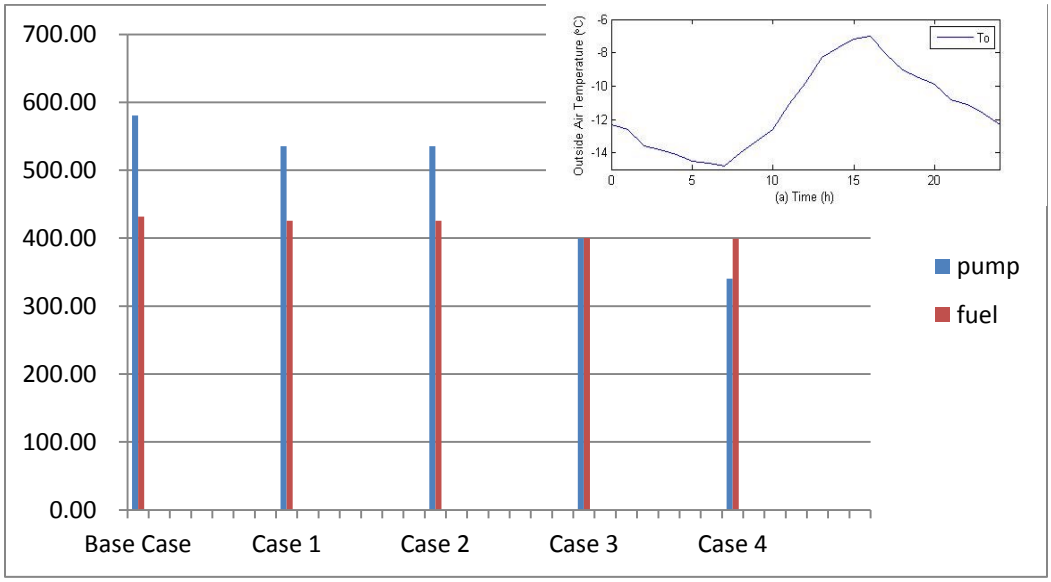

(a) Coldest weather (T_o =-15～-7℃)

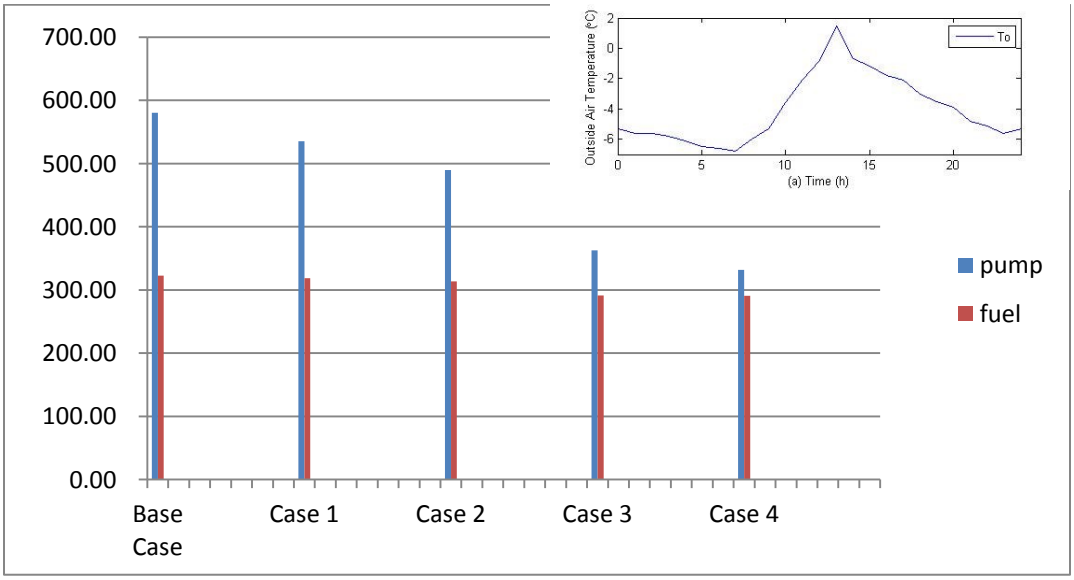

(b) Cold weather (T_o =-7～2℃)

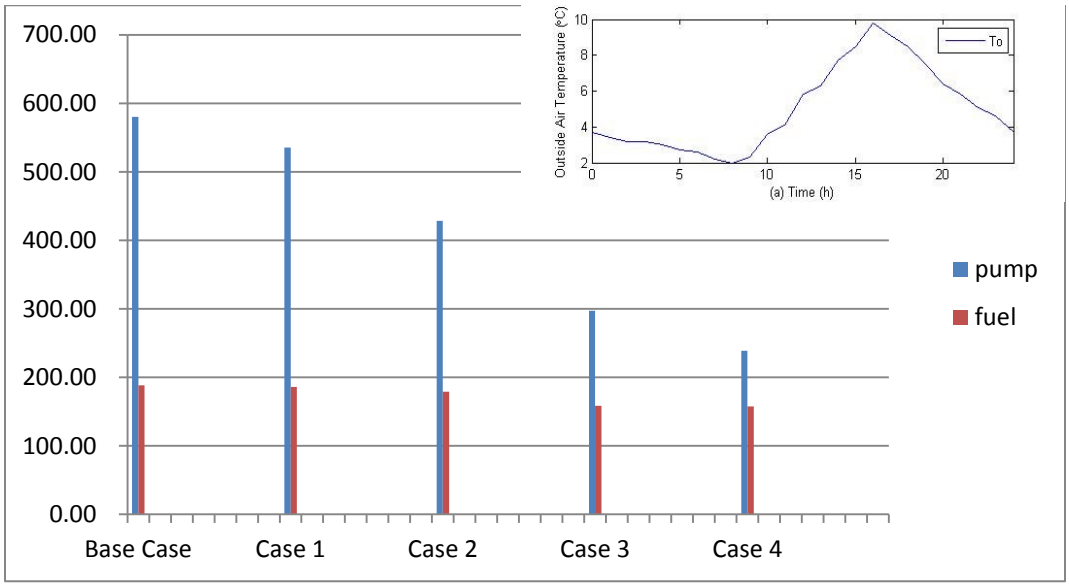

(c) Warm weather (T_o =2～10°C)

Figure 5.9 (a-c) Daily energy consumption under different weather conditions

5.9 Summary

First, a PI control strategy is described in this chapter, to control the boiler water temperature and the zone air temperature under real weather conditions and disturbances. The closed loop simulation results show that response of DH system is satisfied and all temperatures are maintained at their respective set points. In addition, the results show that PI control strategy could save up to 30.6% electrical power energy and 11.5% fuel consumption compared to open loop control.

Second, a multi-variable constrained optimization function was formulated and solved in this chapter. The optimal operating set points such as boiler water temperature and mass flow rate have been found for different weather conditions. Based on the optimal set points near-optimal balance valves opening position have also been found in this chapter. In addition, the simulation results show that the use of optimal set point to control could save more than 19.7% electrical power energy compared to conventional set points which are based on experience and is practiced in most buildings.

Third, by comparing the simulation results of energy consumption under different cases, it is shown that significant saving in energy can be achieved by adjusting the balance valve position as a function of outdoor temperature. The simulation results show that the adjustment of balance valve opening according to outdoor air temperature could save more than 19.9% electrical energy compared to constant opening position.

CHAPTER 6

Contributions, Conclusions, and Recommendations for Future work

6.1 Contributions and conclusions

The contributions of this thesis are in the area of system design, thermal and hydraulic modeling, selecting proper balance valve opening and control strategies for energy efficiency in district heating systems (DH system). The specific contributions and conclusions in these areas are summarized as below.

6.1.1 Modeling of DH systems

(1) A typical district heating system has been designed using steady state design methods. The overall system consists of 5 residential buildings and 1 commercial building.

(2) A dynamic model for the whole DH system which describes the energy transfer processes from heat source to user terminal has been developed. This model includes the sub system models of boiler, supply and return water, zone, heater and exterior walls of the buildings.

(3) Dynamic responses of whole DH system were simulated. The simulation runs correspond to design conditions and real weather conditions which include heat losses such as water leakage, losses from pipe network and disturbances such as solar radiation, internal heat gain, etc.

(4) The open loop simulation results show the relationship between the outdoor air temperature, zone air temperature, water temperature, and water mass flow rate. The results established the output ranges and their trends as a function of outdoor temperature.

6.1.2 Hydraulic system model

(1) A hydraulic model of DH system has been built by using steady state methods to study the water pressure distribution in whole pipe network.

(2) Water pressure drops across the balance and control valves of the pipe network were determined and studied under different hydraulic conditions.

(3) The relationship between outdoor air temperature and balance valve opening was developed by combining dynamic thermal transfer model and the steady state hydraulic model.

(4) The balance valve performance was evaluated in terms of valve opening position at different outdoor air temperatures.

6.1.3 Control strategies and energy optimal operation of DH systems

(1) A PI control strategy was designed to control zone air temperature and boiler water temperature.

(2) The optimization program for energy savings in DH system was developed and the optimal parameters such as water temperature and mass flow rate were calculated for different weather conditions.

(3) The simulation results show that PI control strategy could save more than 30.6% electrical power energy and 11.5% fuel consumption compared to open loop system with no control.

(4) The simulation results show that the use of optimal balance valve opening set points could save more than 19.7% electrical power energy compared to fixed balance valve positions that are widely used.

6.2 Recommendations for future research

Research results conducted in this thesis present opportunity for further developments in control strategy study and optimal operation of DH systems.

(1) The balance valves on the loops may be controlled automatically by controllers in order to improve responses of DH system as a function of seasonal changes in outdoor air temperature.

(2) A variable speed frequency controller may be added on the circulating pump to improve the energy efficiency.

(3) The makeup water pump may be controlled to keep a constant pressure differential in the system to keep constant make up water level.

(4) Improving control strategy for zone air temperature control when significant fluctuations in internal heat gains occur in buildings is recommended.

References

[1] ASHRAE, ASHRAE Handbook-HVAC Systems and Equipment 2008, American Society of Heating, Refrigerating and Air-Conditioning Engineers, Atlanta, 2008

[2] Baoping Xu, Lin Fu & Hongfa Di, Field investigation on consumer behaviour and hydraulic performance of a district heating system in Tianjin, China, *Building and Environment*, 44(2009)249–259

[3] Baoping Xu, Lin Fu, Hongfa Di, Dynamic simulation of space heating systems with radiators controlled by TRVs in buildings, *Energy and Buildings*, 40 (2008), 1755–1764

[4] Claudio Garcia, Comparison of friction models applied to a control valve, *Control Engineering Practice*, 16 (2008), 1231–1243

[5] Faye C. Mc Quiston, Jerald D. Parker, Jeffrey D. Spitler, Heating,Ventilating, and Air conditioning Analysis and Design, 6th edition, John Wiley & Sons, Inc., 2005, New York

[6] Fu Lin, Jiang Yi, Yuan Weixing & Qin Xuzhong. Influence of supply and return water temperatures on the energy consumption of a district cooling system. *Applied Thermal Engineering*, 21 (2001) 511-521

[7] He Ping, Sun Gang, Heat-supply Engineering, 3th edition, China Construct Industry Press, 1993;

[8] Kemal Comakli, BedriYuksel & Omer Comakli, Evaluation of energy and energy losses in district heating network, *Applied Thermal Engineering*, 24 (2004), 1009–1017

[9] Kyu Nam Rhee, Myoung Souk Yeo, Kwang Woo Kim, Evaluation of the control performance of hydronic radiant heating systems based on the emulation using hardware-in-the-loop simulation, *Building and Environment*, 46 (2011), 2012-2022

[10] Li, LianZhong, Dynamic Modeling and Optimal Operation of District Heating Systems. Department of Building, Civil and Environmental Engineering, Concordia University, Theses (M. A. Sc.), 2003;

[11] L. Lianzhong and M. Zaheeruddin, Dynamic modeling and fuzzy augmented PI control of a high-rise building hot water heating system, *Energy for Sustainable Development*, Volume XII, No. 2, June 2008

[12] M.A.A. Shoukat Choudhury, N.F. Thornhill, S.L. Shah, Modelling valve stiction, *Control Engineering Practice*, 13 (2005), 641–658

[13] Mamson AG, Cavitation in Control Valves, Mamson, weismullerstrabe 3, 60314 Frankfurt, Germany

[14] Manohar R. Kulkarni, Feng Hong, Energy optimal control of a residential space-conditioning system based on sensible heat transfer modeling, *Building and Environment*, 39 (2004), 31 – 38

[15] Masoneilan, Masoneilan Control Valve Sizing Handbook, Valve Division, Dresser, Houston, USA

[16] Mauro Gamberi, Riccardo Manzini, Alberto Regattieri, Simulink simulator for building hydronic heating systems using the Newton – Raphson algorithm, *Energy and Buildings*, 41 (2009), 848 – 855

[17] M. Bojic, N. Trifunovic, Linear programming optimization of heat distribution in a district-heating system by valve adjustments and substation retrofit, *Building and Environment*, 35 (2000), 151-159

[18] M. Bojic, N. Trifunovic, S.I. Gustafsson, Mixed 0–1 sequential linear programming optimization of heat distribution in a district-heating system, *Energy and Buildings*, 32(2000), 309–317

[19] M. Zaheer-uddin & P. Monastiriakos, Hydronic Heating Systems: Transient Modeling, Validation and Load Matching. *International Journal of Energy Research*, 22 (1998), 33-46

[20] NurdanYildirim, MacitToksoy, Gulden Gokcen, Piping network design of geothermal district heating systems: Case study for a university campus, *Energy*, 35 (2010), 3256-3262

[21] Takeyoshi Kimura, Takaharu Tanaka, Kayo Fujimoto, Kazuhiko Ogawa, Hydrodynamic characteristics of a butterfly valve - *Prediction of pressure loss characteristics*, ISA Transactions, 34 (1995), 319-326

[22] Tianzhen Hong and Yi Jiang, A New Multizone Model for the Simulation of Building Thermal Performance, *Building and Environment*, Vol. 32, No. 2. pp. 123-128, 1997

[23] Val-Matic, Cavitation in Valves, Val-Matic Valve and Manufacturing corp., 905 Riverside Drive, Elmhurst, IL 60126

[24] Vladimir D. S., Sanja P., B. M., B. Z., &S. N., Efficient Numerical Method for District Heating System Hydraulics. *Energy Conversion and Management*, 48 (2007), 1536-1543

[25] Vladimir D. Stevanovic, BranislavZivkovic, SanjaPrica, BlazenkaMaslovaric,

VladanKaramarkovic, VojinTrkulja, Prediction of thermal transients in district heating systems, *Energy Conversion and Management*, 50 (2009), 2167–2173

[26] Wen Zhen Huang, M. Zaheer-uddin, S.H. Cho, Dynamic simulation of energy management control functions for HVAC systems in buildings, *Energy Conversion and Management*, 47 (2006), 926–943

[27] Zheng Guorong, Dynamic Modeling and Global Optimal Operation of Multi-zone Variable Air Volume HVAC Systems, Concordia University, Centre for Building Studies, Theses (Ph. D.), 1997

[28] Z. Liao, A.L. Dexter, The potential for energy saving in heating systems through improving boiler controls, *Energy and Buildings*, 36 (2004), 261–271

[29] Z. Liao and A.L. Dexter, An inferential control scheme for optimizing the operation of boilers in multi-zone heating systems, *Building Services Eng. Res. Technol. 24*,4 (2003) pp. 245–256

[30] Z. Liao and A.L.Dexter, A simplified physical model for estimating the average air temperature in multi-zone heating systems, *Building and Environment*, 39 (2004), 1013 – 1022

[31] Z. Liao, M. Swainson, A.L. Dexter, On the control of heating systems in the UK, *Building and Environment*, 40 (2005), 343–351

[32] Lyons, J.L., Lyon's Valve Designer's Handbook, Van Nostrand Reinhold Co., 1982